

---

# ROBUST-MULTI-TASK GRADIENT BOOSTING \*

---

**Seyedsaman Emami**  
Escuela Politécnica Superior  
Universidad Autónoma de Madrid  
Madrid

**Gonzalo Martínez-Muñoz**  
Escuela Politécnica Superior  
Universidad Autónoma de Madrid  
Madrid

**Daniel Hernández-Lobato**  
Escuela Politécnica Superior  
Universidad Autónoma de Madrid  
Madrid

## ABSTRACT

The objective of this study is to develop a robust boosting framework capable of handling heterogeneous and outlier tasks in Multi-Task Learning (MTL). Conventional MTL methods assume strong relatedness among tasks, which often fails in real-world scenarios involving adversarial or unaligned tasks that degrade performance. To address this limitation, we propose Robust Multi-Task Gradient Boosting (R-MTGB), a novel ensemble framework that explicitly models task heterogeneity within the gradient boosting paradigm. The methodology structures learning into three sequential stages: (1) shared representation learning to extract common patterns across tasks, (2) outlier-aware partitioning using a learnable task-specific parameter to separate and reweight outlier and non-outlier tasks, and (3) task-specific fine-tuning to refine individual predictors. Extensive experiments on both synthetic and real-world datasets demonstrate that R-MTGB consistently improves predictive accuracy, effectively identifies outlier tasks, and enhances generalization compared to state-of-the-art methods. The achieved results confirm that R-MTGB not only ensures robust performance and interpretability through task-level outlier scores but also provides a scalable and principled framework for reliable multi-task learning in heterogeneous environments.

**Keywords** Multi-Task Learning · Gradient Boosting · Outlier Detection

---

\*This manuscript is currently under review at \*Expert Systems With Applications\*.

## List of Abbreviations

<b>BTAMDL</b>	Boosting Tree-Assisted Multi-Task Deep Learning
<b>CD</b>	Critical Distance
<b>DNN</b>	Deep Neural Network
<b>DP</b>	Data Pooling
<b>DTR</b>	Decision Tree Regressor
<b>FL</b>	Federated Learning
<b>GB</b>	Gradient Boosting
<b>MAE</b>	Mean Absolute Error
<b>MDL</b>	Multi-Task Deep Learning
<b>ML</b>	Machine Learning
<b>MTGB</b>	Multi-Task Gradient Boosting
<b>MTL</b>	Multi-Task Learning
<b>R-MTGB</b>	Robust-Multi-Task Gradient Boosting
<b>RMSE</b>	Root Mean Squared Error
<b>ST</b>	Single-Task
<b>TaF</b>	Task-as-Feature
<b>TS</b>	Task-wise Split

## 1 Introduction

Machine Learning (**ML**) models are increasingly used in scenarios that require learning multiple prediction tasks at the same time. This approach, referred to as Multi-Task Learning (**MTL**), involves learning multiple related or unrelated tasks simultaneously by transferring knowledge from one task to another [Zhang and Yang, 2022]. The main objective of **MTL** is to improve generalization performance by utilizing task-specific information and leveraging shared representations across tasks [Caruana, 1997]. **MTL** has demonstrated significant potential in areas such as computer vision [Shen et al., 2024, Souček et al., 2024] and healthcare [Liu et al., 2024b, Tsai et al., 2025]. By exploiting shared structures across tasks, **MTL** often achieves better generalization compared to training separate models for each task. However, practical applications frequently involve noisy, diverse, or even adversarial task environments, making robustness an essential consideration. In such cases, conventional **MTL** models can experience substantial performance degradation when some tasks are corrupted, poorly defined, or entirely unrelated to the other tasks [Yu et al., 2007].

Beyond **MTL**, Gradient Boosting (**GB**) variants have become one of the most effective techniques in supervised learning, especially when applied with decision trees [Zięba et al., 2016, Chen and Guestrin, 2016, Bentéjac et al., 2021, Shwartz-Ziv and Armon, 2022]. Specifically, **GB** fits a function that explains the target values associated to each input. This function is obtained by combining several predictors, each one obtained by performing a gradient step in function space minimizing a particular loss function [Friedman, 2001]. Building on this success, Multi-Task **GB** extends the **GB** framework to handle multiple related learning tasks simultaneously. For this, a function is fit for each task. Importantly, however, such a function is obtained as the sum of two functions. Namely, a common function that captures the shared structure among tasks, and a task-specific function that accounts for task-specific deviations [Chapelle et al., 2011, Emami et al., 2023]. This formulation enables implicit data sharing and acts as a regularizer, improving generalization—particularly when tasks are similar but not identical. Unlike Single-Task (**ST**) learning, which ignores potential synergies between tasks, or Data Pooling (**DP**), which treats all tasks as identical, multi-task boosting leverages shared structure while respecting task heterogeneity. Empirical results have shown that this method consistently outperforms standard boosting approaches in scenarios where tasks are moderately related [Zhang and Yeung, 2012, Bellot and van der Schaar, 2018, Emami et al., 2023].

Critically, the multi-task variants of **GB**, such as Multi-Task Gradient Boosting (**MTGB**), rely on the key assumption of a shared function across all tasks [Emami et al., 2023]. This need not be the case when some of the tasks are outlier tasks, *i.e.*, they are tasks that do not share any relation with the other tasks. Outlier tasks simply differ significantly

from the other tasks and may deteriorate the **MTL** process. As a matter of fact, in real-world **MTL** scenarios, tasks often exhibit significant heterogeneity [Yu et al., 2007, Gong et al., 2012], reducing the effectiveness of standard **MTL** approaches [Yu et al., 2007]. Under such conditions, the performance of methods like **MTGB** can be severely impaired. Therefore, robustness to outlier tasks and to variations in task difficulty or data quality becomes a critical feature of **MTL** methods. Notwithstanding, robust techniques for **MTL** based on **GB** remain largely unexplored.

In this paper, we propose a novel multi-task boosting algorithm called Robust-Multi-Task Gradient Boosting (**R-MTGB**), that can learn across tasks with varying degrees of relatedness. **R-MTGB** introduces a structured ensemble learning framework composed of three sequential blocks. In the first block, the model learns a global shared representation that captures commonalities across all tasks. The second block distinguishes between outlier and non-outlier tasks by optimizing a regularized task-specific parameter jointly. This enables adaptive weighting of task contributions and mitigates the influence of outlier tasks on the shared function. Finally, the third block performs fine-tuning by learning task-specific predictors, enabling the model to capture the nuances of individual tasks. Importantly, however, the level of contribution of each block to the overall learning process can be adjusted to the observed data. For this, one simply has to change the number of boosting predictors used in that particular block. To be specific, the number of predictors used in each block is a hyperparameter that can be tuned, e.g., using a cross-validation grid search. This modular design allows **R-MTGB** to dynamically balance shared-learning and task-specific adaptation, improving generalization across heterogeneous task sets. As a result, the model is robust to outlier tasks. Besides this, it is also scalable to large datasets, and adaptable to a wide range of loss functions. Finally, **R-MTGB** not only improves robustness and generalization performance, but also enhances interpretability by allowing the clustering of tasks into non-outlier and outlier categories based on the results of the learning process.

The key contributions of this study are as follows:

- **A novel integration of outlier task detection into gradient boosting for multi-task learning:** Unlike previous boosting-based **MTL** methods, task-level outlier-aware partitioning is incorporated directly into the boosting iterations, enabling adaptive emphasis on informative tasks during training.
- **A principled three-stage design developed for heterogeneous task environments:** A sequential architecture comprising shared representation learning, outlier-aware task partitioning, and task-specific refinement, is introduced, theoretically motivated, and empirically validated. This design balances generalization through shared patterns and specialization via per-task refinement, while remaining robust to outlier tasks.
- **A unified boosting formulation that generalizes existing models:** It is shown that several established approaches emerge as special cases of the proposed model when certain components are omitted, highlighting its role as a flexible generalization rather than a simple combination of existing methods.
- **Extensive empirical validation with robustness analysis:** The proposed approach improves predictive accuracy and produces interpretable task-level outlier scores across synthetic and real-world benchmarks.

Collectively, these innovations enable **R-MTGB** to bridge the gap arising from the lack of robust multi-task boosting methods capable of handling heterogeneous and outlier tasks. Traditional multi-task boosting frameworks, such as **MTGB**, assume a uniform degree of relatedness among tasks and thus become vulnerable when confronted with unaligned tasks. **R-MTGB** overcomes this limitation through an automatic outlier detection mechanism that assigns extreme, opposite weights to outlier and non-outlier tasks. This mechanism allows the model to automatically separate and adapt to heterogeneous task behaviors, reducing the disruptive influence of anomalous tasks while preserving the shared structure among related ones. Consequently, **R-MTGB** provides a unified boosting framework that achieves robustness and interpretability without sacrificing predictive accuracy.

The remainder of this paper is structured as follows. Section 2 reviews prior studies on **MTL**, **GB**, and multi-task boosting frameworks, highlighting their limitations and comparing them with the proposed approach. Section 3 introduces the developed methodology, including its mathematical foundations and theoretical analysis. Section 4 presents the experiments conducted on both synthetic and real-world datasets, along with a detailed discussion of the results. Finally, Section 5 concludes the study with a summary of the key findings.

## 2 Related Work

This section reviews prior work relevant to the proposed approach. We begin by introducing the core ideas and categories of **MTL** in Subsection 2.1. In Subsection 2.2, we summarize the development of **GB** and its variants. Finally, in Subsection 2.3, we discuss prior attempts to apply boosting methods to **MTL** problems and highlight the differences between these approaches and ours.

## 2.1 Multi-Task Learning

MTL is an ML approach in which multiple tasks are learned simultaneously, allowing shared knowledge across functions to improve overall performance [Caruana, 1997]. The core assumption in MTL is that tasks within a given dataset are related [Caruana, 1997, Li et al., 2015]. By leveraging transfer learning, MTL enables models to use information gained from one task to enhance learning and generalization on related tasks, leading to more robust and adaptable systems compared to training separate models for each task [Zhang and Yang, 2022].

Several well-defined approaches to exploring MTL have been studied, including feature learning, low-rank parameterization, task clustering, task relationship modeling, and decomposition methods [Zhang and Yang, 2022]. In feature learning, the objective is to discover a shared representation across multiple tasks by leveraging shared features. This approach has been implemented in various ML models, including neural networks [Caruana, 1997, Liao and Carin, 2005] and deep neural networks [Zhang et al., 2014, LI et al., 2014, Liu et al., 2015, Zhang et al., 2015].

The Low-Rank methodology, on the other hand, is designed to capture the relatedness among tasks by assuming that the parameter matrix across tasks lies in a low-rank subspace [Ando et al., 2005]. This implies the existence of shared latent factors among tasks. The objective is to minimize a joint loss function over the weight matrix, subject to a low-rank constraint (often via nuclear norm regularization or matrix factorization). Recent studies have applied this approach to develop MTL approaches in various areas, such as improving parameter-efficient training of multi-task models [Agiza et al., 2024], identifying outliers [Chen et al., 2011], and reconstructing low-rank weight matrices [Han and Zhang, 2016].

Another approach in MTL involves grouping related tasks into clusters, as first proposed by Thrun and O’Sullivan [1996], where it exploits the shared structure within each cluster to enhance learning. Later, a theoretical framework for MTL based on clustering tasks and assigning each cluster to one of a limited number of shared hypotheses was proposed [Crammer and Mansour, 2012]. This hard-assignment strategy facilitates learning from limited data while effectively controlling model complexity.

Another category in MTL focuses on approaches that encourage the model to treat the average of task-specific parameters as a central assumption, based on the idea that tasks are inherently similar [Evgeniou and Pontil, 2004, Parameswaran and Weinberger, 2010]. Other studies regularize the objective function by measuring pairwise task similarities [Evgeniou et al., 2005] or controlling task relatedness [Kato et al., 2007].

Lastly, the decomposition approach involves breaking down model parameters into shared and task-specific components. This enables the model to learn shared patterns across tasks while also capturing nuances unique to individual tasks. A study by Han and Zhang [2015] introduced an approach that simultaneously learns both shared and task-specific parameters directly from data by implementing a layered decomposition of the parameter matrix, with each layer representing a level in the task hierarchy. Another study decomposes the model parameters for each task into shared components and task-specific deviations, applying a methodology to learn multiple related parameters tasks simultaneously [Evgeniou and Pontil, 2004]. This approach allows for better control over the shared information, with each task parameter vector represented as the sum of a shared vector and a task-specific offset. In a related line of work, but using a different ML model, MTGB was introduced [Emami et al., 2023]. This approach explicitly incorporates both shared and task-specific components through a two-phase process. In the first phase, a common set of models is trained to capture patterns shared across all tasks. In the second phase, separate models are added for each task to learn the pseudo-residual information specific to that task.

Recent advancements in MTL have been primarily fueled by deep learning frameworks capable of capturing hierarchical and shared representation [Zhang and Yang, 2022]. These approaches can generally be classified into three primary categories. The first category focuses on learning a unified feature representation across multiple tasks by sharing the initial layers of the network [Zhang et al., 2014, Liu et al., 2015, Zhang et al., 2015, LI et al., 2014]. The second category employs adversarial learning techniques to obtain a common representation suitable for multiple tasks [Shinohara, 2016]. The third category, represented by the cross-stitch network, aims to learn distinct yet interrelated feature representations for different tasks [Misra et al., 2016].

Despite the successes of deep learning-based MTL methods in domains such as computer vision [Vandenhende et al., 2022, Fontana et al., 2024] and natural language processing [Liu et al., 2018, Chen et al., 2024], these architectures inherit some of the same limitations when applied to tabular data. In particular, multiple recent studies show that neural-network approaches often underperform tree-ensemble or boosting methods on standard tabular classification and regression benchmarks, and require heavier hyperparameter tuning, more training effort, and less interpretability than ensemble-based methods [Grinsztajn et al., 2022, McElfresh et al., 2023, Borisov et al., 2024]. These limitations carry over into MTL settings: when tasks involve outlier tabular data, a deep MTL model may struggle to extract the correct inductive biases or to adapt to outlier tasks, potentially resulting in sub-optimal performance [Aoki et al., 2022, Malhotra et al., 2023]. Hence, MTL frameworks based purely on deep networks may be less optimal in tabular data

environments compared to ensemble-based methods such as boosting ensembles [Zhang and Li, 2019, Jiang et al., 2020a].

## 2.2 Gradient Boosting

In the context of tabular datasets and supervised learning models, ensemble learning has demonstrated strong performance in solving a wide range of **ML** problems [Shwartz-Ziv and Armon, 2022], including classification and regression [Zieba et al., 2016, Lakshminarayanan et al., 2017, He et al., 2018, Xia and Bouganis, 2023, Özyüksel Çiftçioğlu, 2024]. Ensemble models work by combining multiple base learners to construct a more robust and accurate final model [Zhou, 2012, Khan et al., 2024].

**GB** is among the most successful ensemble methods. It builds predictive models by sequentially adding base learners (typically Decision Tree Regressor (**DTR**)) to correct the residuals of preceding models [Friedman, 2001]. This results in a learning process that minimizes a loss function by performing gradient descent in functional space. More precisely, adding each new predictor can be seen as a step in functional space with the goal of minimizing the loss function (*i.e.*, the squared error for regression or the cross-entropy for classification). The result of the learning process is a function from inputs to targets that is optimal according to the particular loss function employed.

A faster variant of **GB** is XGBoost, which introduces regularization into the objective function and employs an improved branch-splitting method in **DTR**, resulting in faster training and enhanced accuracy [Chen and Guestrin, 2016]. Another notable advancement is LightGBM, which accelerates **GB** through novel sampling strategies and feature bundling methods, achieving high speed and performance [Ke et al., 2017]. CatBoost, further addresses prediction shifts in **GB** by introducing a permutation-based technique [Prokhorenkova et al., 2018].

The strong performance of **GB** has led to the development of multi-class classification and multi-output regression models. These models extend **GB** and its variants to address such problems more efficiently by restructuring **GB** variants to support multi-output and multi-class problems within their loss functions and base learners. Gradient-Boosted Decision Trees for Multiple Outputs represents the multi-output extension of XGBoost [Zhang and Jung, 2021], while Condensed-Gradient Boosting is a multi-output version of **GB** that employs multi-output **DTR** [Emami and Martínez-Muñoz, 2025], which is also less complex than previous **GB** variants in terms of both time and space requirements. These developments highlight flexibility and potential of **GB** framework for tackling more complex supervised learning problems involving multiple tasks.

## 2.3 Boosting Multi-Task Learning

The first study to propose a multi-task boosting approach is Chapelle et al. [2011], where the authors employed **GB** to design a customized **MTL** framework. Their method maintains  $T + 1$  base learners composed of (**DTRs**): one global model to capture shared structure among all tasks and  $T$  task-specific models to account for individual task nuances. At each boosting iteration, the algorithm adds a new base learner to either the global or a task-specific model, depending on which yields the greatest reduction in the overall objective, determined via steepest descent.  $\ell_1$ -norm regularization is employed to promote sparsity in the learned functions. The overall objective is to iteratively optimize a shared loss function across tasks by selecting the direction (*i.e.*, base learner and task) that most improves the loss, as approximated through a first-order Taylor expansion.

Another boosting-based **MTL** framework is Boosting Tree-Assisted Multi-Task Deep Learning (**BTAMDL**), which integrates **DTR** with Deep Neural Network (**DNN**) [Jiang et al., 2020b]. The boosting process is implemented in two distinct stages. In the first stage, a Multi-Task Deep Learning (**MDL**) network is trained on several related tasks to learn shared representations, thereby leveraging data-rich tasks to support those with limited data. In the second stage, the output of the final hidden layer of the **MDL** network is used as input features for training a **GB** model.

Another study similar to the one proposed in Chapelle et al. [2011] is **MTGB**. However, **MTGB** differs in structure, framework, and optimization strategy [Emami et al., 2023]. Specifically, **MTGB** builds on **GB** by explicitly separating the learning process into two stages. First, learning a shared function for each task by fitting shared base learners across tasks. Second, learning a task-specific function for each task by fitting task-specific base learners. The final function used to predict targets given inputs for each task is a combination of the two aforementioned functions. In summary, the optimization (carried out using gradient descent in the functional space) is performed in two phases: first, a shared loss function is minimized using the combined data from all tasks; then, task-specific loss functions are optimized separately for each task. A limitation of this work is that outlier tasks, which significantly differ from the other tasks by sharing no information at all with them, may deteriorate the process of fitting the shared function described above.

Table 1: Comparison of boosting-based **MTL**. (Symbols:  $\checkmark$  = present;  $\times$  = absent).

Method	Shared Rep.	Task-specific Modeling	Outlier Task Handling
Boosted <b>MTL</b> [Chapelle et al., 2011]	$\checkmark$	$\checkmark$	$\times$
<b>MTGB</b> [Emami et al., 2023]	$\checkmark$	$\checkmark$	$\times$
<b>BTAMDL</b> [Jiang et al., 2020b]	$\checkmark$	$\checkmark$	$\times$
FederBoost [Liu et al., 2024a]	$\checkmark$ (global)	$\checkmark$ (local)	$\times$
<b>TS-GB</b> [Chen et al., 2021]	$\checkmark$ (shared tree)	$\checkmark$ (splits adapted)	$\times$
<b>R-MTGB</b> (Ours)	$\checkmark$	$\checkmark$	$\checkmark$

An alternative approach that differs significantly from previous studies is Boosted-**MTL** framework, which is based on a Federated Learning (**FL**) paradigm [Liu et al., 2024a]. This framework operates in two sequential stages. First, in the *global learning* stage, multiple districts collaborate through a privacy-preserving federated **GB** scheme, known as FederBoost, to learn shared load patterns. Second, in the *local learning* stage, each district independently fine-tunes a local model to capture its district-specific load characteristics. The final model is constructed as the sum of the global and local **GB** models.

In contrast to restructuring the **GB** framework, Task-wise Split (**TS**)-**GB** introduced a task-specific splitting mechanism for **DTR** [Chen et al., 2021], replacing the standard criterion with one based on task-specific performance, termed task gain. A split is performed only when the negative impact on other tasks does not exceed a predefined threshold. Later, an extension of **TS-GB** was introduced to address the issue of imbalanced data by proposing two approaches: **TS-GB** $_{\beta}$ , which revises the task gain ratio to be more sensitive to the number of affected tasks rather than the number of instances; and **TS-GB** $_{\kappa}$ , which reweights datasets using a softmax-based method to balance data distribution across tasks [Ma et al., 2022]. These adaptations enhance both overall and task-specific prediction performance without compromising the accuracy for minority labels, as reported in a recent preprint [Ying et al., 2022].

## 2.4 Comparative analysis

Our proposed method falls into the first category of boosting-based **MTL** approaches. However, unlike tree-based models or the **FL** framework, our method redefines the ensemble structure to directly address challenges specific to **MTL**. Importantly, while prior work in this category has largely focused on modeling shared and task-specific patterns, they have not addressed the presence of outlier or adversarial tasks, which can degrade overall model performance. Table 1 summarizes key design choices across representative boosting-based **MTL** methods. Specifically, we compare whether a method explicitly (i) learns a *shared representation* across tasks, (ii) models *task-specific* components, and (iii) handles *outlier/adversarial tasks within the GB fitting process*. The table shows that the proposed approach, **R-MTGB**, is the only one fulfilling the three considered criteria.

Existing boosting-based **MTL** methods primarily decompose the predictor into a shared part and per-task components, and then decide where to add base learners (e.g., global vs. task-specific in Chapelle et al. [2011] or Emami et al. [2023]). **BTAMDL** [Jiang et al., 2020b] introduces an **MDL**-based regularization to balance global and task-specific learners. This encourages careful information sharing, but does not explicitly identify adversarial or outlier tasks. **TS-GB** [Chen et al., 2021] addresses the negative task transfer problem by constraining tree splits at the node level, thereby reducing harmful feature-wise splits. Nevertheless, it does not *learn* a notion of task outlierness nor it reweights task contributions during **GB** training. Therefore, its robustness is heuristic rather than adversarial-task driven. **FL** variants such as FederBoost [Liu et al., 2024a] combine global collaboration (distributional via **FL**) with local refinement, improving privacy and distributional robustness. Yet, they also do not *jointly optimize* any task-outlier variable that influence each base learner contributions inside boosting. This reveals a clear research gap in the current literature: while existing multi-task boosting methods can model shared and task-specific information, none can automatically identify and adapt to outlier or adversarial tasks within the boosting process. By contrast, our proposed method, **R-MTGB**, incorporates a learnable mechanism, parameterized within the boosting loop, which enables a soft partition of tasks into outlier and non-outlier components. Thus, **R-MTGB** provides principled robustness against adversarial or outlier tasks and does not rely on heuristic adjustments. Consequently, outlier tasks are down-weighted where they would corrupt the shared structure among related tasks, yet, each task still benefits from task-specific fine-tuning. To our knowledge, no prior **GB**-based **MTL** approach learns such an *task-specific parameter* that (i) detects outlier tasks *during* boosting and (ii) adapts their learning process to a separate component, thereby providing principled robustness to task heterogeneity. This not only improves robustness and generalization performance, but also enhances interpretability by allowing the clustering of tasks into non-outlier and outlier categories based on the results of the learning process.

### 3 Methodology

This section details the methodology used in this study. It begins with the preliminaries and notation (Subsection 3.1), followed by an introduction to **MTL** (Subsection 3.2). Next, an overview of **GB** framework is provided (Subsection 3.3), leading to the presentation of the proposed **R-MTGB** extension and its underlying mathematical framework (Subsection 3.4). Finally, a theoretical analysis is presented (Subsection 3.5).

#### 3.1 Preliminaries and Notation

In this study, we define the input space as  $\mathcal{X} \subseteq \mathbb{R}^d$ , where each input  $\mathbf{x} \in \mathcal{X}$  is a  $d$ -dimensional feature vector. The corresponding output space is  $\mathcal{Y} \subseteq \mathbb{R}$ , where each output  $y \in \mathcal{Y}$  is a target scalar value, in the case of regression problems. In the case of classification we consider a one-hot encoding scheme for the targets, *i.e.*,  $\mathcal{Y} \subset \{0, 1\}^K$ , with  $K$  the number of classes. The dataset is denoted by  $\mathcal{D} = \{(\mathbf{x}_i, y_i)\}_{i=1}^N$ , where each sample  $(\mathbf{x}_i, y_i)$  is drawn independently and identically distributed (i.i.d.) from  $P(\mathcal{X}, \mathcal{Y})$ , and  $N$  is the number of samples. This corresponds to a supervised learning setting, where the goal is to learn a mapping from inputs to outputs using labeled data [Cunningham et al., 2008].

Subsequently, to evaluate the performance of the training model, we define a loss function  $\mathcal{L}(y, \hat{F})$ , which measures the discrepancy between the true output  $y$  and the model's output  $\hat{F}$ . The specific form of the loss function depends on the nature of the problem [Wang et al., 2022a]. In this study, we use the cross-entropy loss function for classification,

$$\mathcal{L}(\mathbf{y}, \hat{\mathbf{F}}) = - \sum_{k=1}^K y_k \ln(P_k), \quad (1)$$

where  $K$  is the number of distinct class labels,  $\mathbf{y}$  is a one-hot encoded vector of length  $K$ , and  $P_k$  is the predicted probability of class  $k$ ,

$$P_k = \frac{\exp(\hat{F}_k)}{\sum_{k=1}^K \exp(\hat{F}_k)}. \quad (2)$$

Furthermore,  $\hat{\mathbf{F}}$  is a vector of length  $K$  with the specific model's output for each of the  $K$  class labels associated to the corresponding inputs  $\mathbf{x}$ .

For regression, we employ the squared error loss function,

$$\mathcal{L}(y, \hat{F}) = \frac{1}{2} (y - \hat{F})^2, \quad (3)$$

where  $y$  is the observed target and  $\hat{F}$  is the model's output for the input  $\mathbf{x}$ .

#### 3.2 Multi-Task Learning

Considering a collection of  $T$  tasks, each task  $t \in \{1, \dots, T\}$  is associated with its own input-output space,  $\mathcal{X}_{(t)}$  and  $\mathcal{Y}_{(t)}$ , respectively. We assume a shared input space  $\mathcal{X} = \mathcal{X}_1 = \dots = \mathcal{X}_T$ , with consistent input feature dimensionality  $d^{(t)} = d$  across all tasks. Similarly, the output space is shared among tasks,  $\mathcal{Y} = \mathcal{Y}_1 = \dots = \mathcal{Y}_T$ . Each task  $t$  has its own dataset,

$$\mathcal{D}_t = \{(\mathbf{x}_{i,t}, y_{i,t})\}_{i=1}^{N^{(t)}}, \quad (4)$$

where  $(\mathbf{x}_{i,t}, y_{i,t}) \sim P_t(\mathcal{X}_t, \mathcal{Y}_t)$ . While these tasks are generally assumed to be related [Caruana, 1997, Chapelle et al., 2011, Emami et al., 2023], in practice, the collection may contain *outlier tasks* that deviate significantly from the shared (common) structure. Such tasks can negatively impact the quality of the shared representation and degrade overall performance if treated uniformly within the learning process [Gong et al., 2012, Yu et al., 2007].

The goal of **MTL** is to simultaneously learn a collection of task-specific functions [Evgeniou and Pontil, 2004],

$$\{F_t : \mathcal{X}_t \rightarrow \mathcal{Y}_t\}_{t=1}^T,$$

that collectively minimize the total loss across all tasks,

$$F(\mathbf{x}) = \arg \min_{\{\hat{F}_t\}_{t=1}^T} \sum_{t=1}^T \sum_{i=1}^{N^{(t)}} \left[ \mathcal{L} \left( y_{i,t}, \hat{F}_t(\mathbf{x}_{i,t}) \right) \right]. \quad (5)$$

To facilitate parameter sharing across tasks, **MTL** models can alternatively express each task-specific function  $F_t$  as the sum of a shared component and a task-specific component,

$$F_t(\mathbf{x}) = \phi(\mathbf{x}) + \psi_t(\mathbf{x}), \quad (6)$$

where  $\phi : \mathcal{X} \rightarrow \mathcal{Y}$  denotes a *shared function* capturing common structure across tasks, and  $\psi_t : \mathcal{X}_t \rightarrow \mathcal{Y}_t$  is a *task-specific function* modeling individual task characteristics. This additive formulation enables the model to learn a global inductive bias via  $\phi$ , while still allowing per-task flexibility through  $\psi_t$ . However, the presence of outlier tasks, which do not align well with the dominant task structure, can mislead the learning of the shared representation  $\phi$ , resulting in degraded performance across the entire task set.

### 3.3 Gradient Boosting

The primary objective of **GB** model, as introduced by [Friedman \[2001\]](#), is to iteratively minimize a given loss  $\mathcal{L}(y, \hat{F}(\mathbf{x}))$ , by finding a function that maps the input features  $\mathbf{x}$  to the predicted output  $\hat{F}$ ,

$$F(\mathbf{x}) = \arg \min_{\hat{F}(\mathbf{x})} \sum_{i=1}^N \left[ \mathcal{L}(y_i, \hat{F}(\mathbf{x}_i)) \right]. \quad (7)$$

This optimization is performed forward stage-wise by sequentially adding base learners  $h_m(\mathbf{x})$  and incorporating the ensemble parameter  $\gamma$  at each boosting iteration  $m$  to the model,

$$\hat{F}_M(\mathbf{x}) = \sum_{m=0}^M \gamma_m h_m(\mathbf{x}). \quad (8)$$

The model is initialized with a constant value that minimizes the loss,

$$\hat{F}_0(\mathbf{x}) = \arg \min_{\gamma} \sum_{i=1}^N \mathcal{L}(y_i, \gamma). \quad (9)$$

Hence, Eq. (7) can be expressed as a stage-wise greedy process,

$$(\gamma_m, h_m) = \arg \min_{\{\gamma_m, h_m\}} \sum_{i=1}^N \mathcal{L}(y_i, \hat{F}_{m-1}(\mathbf{x}_i) + \gamma_m h_m(\mathbf{x}_i)). \quad (10)$$

At each iteration  $m$ , instead of directly optimizing Eq. (10), **GB** utilizes the negative gradient of the loss function (pseudo-residuals) with respect to the prediction of the current model to guide the learning of the next base learner,

$$r_{i,m} = - \left[ \frac{\partial \mathcal{L}(y_i, \hat{F}(\mathbf{x}_i))}{\partial \hat{F}(\mathbf{x}_i)} \right]_{F=\hat{F}_{m-1}(\mathbf{x}_i)}, \quad (11)$$

for each sample  $i$  in the dataset. A new base learner  $h_m(\mathbf{x})$  is then fitted to these pseudo-residuals by minimizing the squared error (regardless of the loss function the ensemble is trying to optimize),

$$h_m(\mathbf{x}) = \arg \min_{\{h \in \mathcal{H}\}} \sum_{i=1}^N (r_{i,m} - h_m(\mathbf{x}_i))^2, \quad (12)$$

where  $\mathcal{H}$  denotes the hypothesis space of base learners, typically a set of Decision Tree Regressor (**DTR**). Once the base learner  $h_m(\mathbf{x})$  is determined, the optimal parameter  $\gamma_m$  is obtained by solving the line search problem,

$$\gamma_m = \arg \min_{\gamma_m} \sum_{i=1}^N \mathcal{L}(y_i, \hat{F}_{m-1}(\mathbf{x}_i) + \gamma_m h_m(\mathbf{x}_i)). \quad (13)$$

However, in practice, often  $\gamma_m$  is set simply equal to 1.

After  $M$  boosting iterations, the final predictive model is built as an additive ensemble of base learners,

$$F(\mathbf{x}) = \hat{F}_M(\mathbf{x}) = \hat{F}_0(\mathbf{x}) + \eta \sum_{m=1}^M \gamma_m h_m(\mathbf{x}), \quad (14)$$

where  $\eta \in (0, 1]$  is a learning rate, that is used to regularize the gradient descent steps in the learning process. In summary, **GB** simply performs gradient descent in function space by incorporating, at each boosting iteration, a new predictor into the ensemble.

**GB** has consistently shown strong empirical performance across a diverse set of **ML** problems, including regression [Touzani et al., 2018, Zhang et al., 2024], binary and multi-class classification [Taha and Malebary, 2020, Gunasekara et al., 2024], ranking [Plaia et al., 2022], missing value estimation [Samad et al., 2022], and **MTL** problems [Chapelle et al., 2011, Liu et al., 2024a, Emami et al., 2023]. Its flexibility in accommodating different loss functions makes it well-suited for both standard and specialized applications [Natekin and Knoll, 2013, Bentéjac et al., 2021].

### 3.4 Robust Multi-Task Gradient Boosting

To address challenges in **MTL**, such as task heterogeneity and outlier task influence, we propose a three-stage **GB** framework called **R-MTGB**, which integrates robustness and shared representation learning within the **GB** paradigm. The training process of **R-MTGB** model is divided into three sequential blocks, where each block has a specific motivation that progressively refines the learning process: (i) initialize with general knowledge, (ii) enforce robustness against outliers, and (iii) specialize to individual tasks.

- **Block 1 (Shared Representation Learning).** Focuses on shared representation learning by leveraging all tasks jointly to identify a common latent function that captures task-invariant patterns. This prevents *cold-start* bias by providing a strong initialization before any task-specific adaptation.
- **Block 2 (Outlier-Aware Partitioning).** Introduces robustness to task outliers by distinguishing between non-outlier and outlier tasks through a sigmoid-based weighting mechanism. This mechanism assigns extreme weights to outlier tasks, amplifies the contribution of reliable tasks, and suppresses the influence of misaligned ones, thereby enabling the model to focus on the most informative task signals and mitigate negative transfer.
- **Block 3 (Task-Specific Fine-Tuning).** Performs task-specific refinement, where individual models are fine-tuned for each task based on the previously learned shared and robust representations. This allows the recovery of fine-grained task details that joint training may suppress.

Each block builds upon the outputs of the previous blocks, progressively refining the model to improve performance across both related and unrelated tasks. Formally, the total number of boosting iterations  $M$  is partitioned into three phases:

$$M = M_1 + M_2 + M_3,$$

where  $M_1$ ,  $M_2$ , and  $M_3$  correspond to the boosting iterations assigned to Block 1, Block 2, and Block 3, respectively. The number of iterations of each block is a hyperparameter that will be adjusted in practice using a cross-validation grid search.

The final proposed ensemble prediction function for a given input  $\mathbf{x}$  is

$$F_t(\mathbf{x}) = \hat{F}^{(\text{shared})}(\mathbf{x}) + (1 - \sigma(\theta_t)) \cdot \hat{F}^{(\text{non-outlier})}(\mathbf{x}) + \sigma(\theta_t) \cdot \hat{F}^{(\text{outlier})}(\mathbf{x}) + \hat{F}_t^{(\text{task})}(\mathbf{x}), \quad (15)$$

where,

- $\hat{F}^{(\text{shared})}$  is the shared-model that captures global shared structures across all tasks.
- $\hat{F}^{(\text{non-outlier})}$  models patterns characteristic of non-outlier tasks.
- $\hat{F}^{(\text{outlier})}$  captures patterns specific to outlier tasks.
- $\hat{F}_t^{(\text{task})}$  represents the task-specific fine-tuned model for task  $t$ .
- $\sigma(\theta_t) = \frac{1}{1 + \exp(-\theta_t)}$  is the sigmoid function that simply outputs the probability that a task is an outlier task.

Although the ensemble prediction function in Eq. (15) contains four components, they are learned iteratively through 3 training blocks. Specifically, Block 2 *jointly* models both the outlier and non-outlier tasks via a unified regularization mechanism that allocates task-specific weights. This shared optimization process gives rise to two separate components in the second block. Namely,  $\hat{F}^{(\text{outlier})}$  and  $\hat{F}^{(\text{non-outlier})}$ . Importantly, each individual function is obtained by combining the different base learners generated at each block. Namely,

$$\hat{F}^{(\text{shared})}(\mathbf{x}) = \sum_{m=1}^{M_1} \eta h_m^{(\text{shared})}(\mathbf{x}). \quad (16)$$

$$\hat{F}^{(\text{outlier})}(\mathbf{x}) = \sum_{m=1}^{M_2} \eta h_m^{(\text{outlier})}(\mathbf{x}). \quad (17)$$

$$\hat{F}^{(\text{non-outlier})}(\mathbf{x}) = \sum_{m=1}^{M_2} \eta h_m^{(\text{non-outlier})}(\mathbf{x}). \quad (18)$$

$$\hat{F}_t^{(\text{task})}(\mathbf{x}) = \sum_{m=1}^{M_3} \eta h_{m,t}^{(\text{task})}(\mathbf{x}). \quad (19)$$

where  $\eta$  is the learning rate considered and each base learner, denoted by  $h_m^{(\cdot)}$  and  $h_{m,t}^{(\cdot)}$ , is implemented as a **DTR**. In the case of multi-class classification  $h_m^{(\cdot)}$  and  $h_{m,t}^{(\cdot)}$  are multi-output **DTRs**, as in [Emami and Martínez-Muñoz \[2025\]](#). Class probabilities are simply obtained by applying the soft-max activation function.

These base learners are trained in sequence, in an iterative process, at each block, by fitting the pseudo-residuals associated to the current state of the corresponding individual function  $\hat{F}^{(\text{shared})}$ ,  $\hat{F}^{(\text{non-outlier})}$ ,  $\hat{F}^{(\text{outlier})}$  or  $\hat{F}_t^{(\text{task})}$ . This process is equivalent to performing gradient descent in function space, as in the standard **GB** algorithm. More precisely, the corresponding objective that is minimized to fit each  $h_m^{(\cdot)}$  and each  $h_{m,t}^{(\cdot)}$ , at each block, is

$$\mathcal{L}_m^{(\text{shared})} = \sum_{t=1}^T \sum_{i=1}^{N_t} \|h_m^{(\text{shared})}(\mathbf{x}_{i,t}) - r_{i,m,t}^{(\text{shared})}\|_2^2, \quad (20)$$

$$\mathcal{L}_m^{(\text{outlier})} = \sum_{t=1}^T \sum_{i=1}^{N_t} \|h_m^{(\text{outlier})}(\mathbf{x}_{i,t}) - r_{i,m,t}^{(\text{outlier})}\|_2^2, \quad (21)$$

$$\mathcal{L}_m^{(\text{non-outlier})} = \sum_{t=1}^T \sum_{i=1}^{N_t} \|h_m^{(\text{non-outlier})}(\mathbf{x}_{i,t}) - r_{i,m,t}^{(\text{non-outlier})}\|_2^2, \quad (22)$$

$$\mathcal{L}_{m,t}^{(\text{task})} = \sum_{i=1}^{N_t} \|h_{m,t}^{(\text{task})}(\mathbf{x}_{i,t}) - r_{i,m,t}^{(\text{task})}\|_2^2, \quad (23)$$

where  $\mathbf{x}_{i,t}$  is the input for instance  $i$  in task  $t$  and  $r_{i,m,t}^{(\cdot)}$  is the corresponding pseudo-residual at iteration  $m$ .

The pseudo-residuals  $r_{i,m,t}^{(\cdot)}$  are recalculated at every boosting iteration  $m$  for their respective block, for the corresponding number of iterations  $M_1$ ,  $M_2$ , and  $M_3$ . During Block 2, the pseudo-residuals are weighted by a task-specific factor  $\theta_t$  reflecting task relatedness, so that outlier tasks have less influence on the shared component. The weights  $\theta_t$  are learned jointly during Block 2, as described below. In our implementation, the initial ensemble prediction in Eq. (15) is set to zero before any learning occurs. The following paragraphs describe each block in detail.

**Block 1 - shared-Learning via Data Pooling:** In the first block,  $M_1$  shared-level predictors are trained, iteratively, to form a shared set of base learners  $h_m^{(\text{shared})}(\mathbf{x}_i, r_{i,m,t}^{(\text{shared})})$  that constitute  $\hat{F}^{(\text{shared})}(\mathbf{x})$ , as indicated in Eq. (16), using pooled data from all tasks,

$$\mathcal{D}_{\text{pool}} = \bigcup_{t=1}^T \mathcal{D}^{(t)}, \quad (24)$$

and pseudo-residuals computed as,

$$\begin{aligned} r_{i,m,t}^{(\text{shared})} &= -\frac{\partial \mathcal{L}(y_{i,t}, F(\mathbf{x}_{i,t}))}{\partial \hat{F}^{(\text{shared})}(\mathbf{x}_{i,t})} \\ &= -\frac{\partial \mathcal{L}(y_{i,t}, F(\mathbf{x}_{i,t}))}{\partial F(\mathbf{x}_{i,t})} \cdot \frac{\partial F(\mathbf{x}_{i,t})}{\partial \hat{F}^{(\text{shared})}(\mathbf{x}_{i,t})} \\ &= -\frac{\partial \mathcal{L}(y_{i,t}, F(\mathbf{x}_{i,t}))}{\partial F(\mathbf{x}_{i,t})} \end{aligned} \quad (25)$$

That is, the pseudo-residuals in this block are vectors pointing in the negative gradient of the loss with respect to  $\hat{F}^{(\text{shared})}$ . Once a predictor  $h_m^{(\text{shared})}$  has been fitted by minimizing Eq. (20), it is incorporated into  $\hat{F}^{(\text{shared})}$ . This process repeats for  $M_1$  iterations.

**Block 2 - Outlier-Aware Task Partitioning:** To mitigate the impact of task outliers, the second block adopts a two-branch structure over the pooled data ( $\mathcal{D}_{\text{pool}}$ ). One branch targets outlier tasks, while the other focuses on non-outlier tasks. The outlier tasks branch is obtained by fitting  $h_m^{(\text{outlier})}(\mathbf{x}_i, r_{i,m,t}^{(\text{outlier})})$ , to the negative gradient of the loss with respect to  $F^{(\text{outlier})}$ ,

$$\begin{aligned} r_{i,m,t}^{(\text{outlier})} &= -\frac{\partial \mathcal{L}(y_{i,t}, F(\mathbf{x}_{i,t}))}{\partial \hat{F}^{(\text{outlier})}(\mathbf{x}_{i,t})} \\ &= -\frac{\partial \mathcal{L}(y_{i,t}, F(\mathbf{x}_{i,t}))}{\partial F(\mathbf{x}_{i,t})} \cdot \frac{\partial F(\mathbf{x}_{i,t})}{\partial \hat{F}^{(\text{outlier})}(\mathbf{x}_{i,t})}, \end{aligned} \quad (26)$$

which yields,

$$r_{i,m,t}^{(\text{outlier})} = -\frac{\partial \mathcal{L}(y_{i,t}, F(\mathbf{x}_{i,t}))}{\partial F(\mathbf{x}_{i,t})} \cdot \sigma(\theta_t). \quad (27)$$

That is, the pseudo-residuals in this branch of the second block (Block 2a) are vectors pointing in the negative gradient of the loss with respect to  $\hat{F}^{(\text{outlier})}$ . Once a predictor  $h_m^{(\text{outlier})}$  has been fitted by minimizing Eq. (21), it is incorporated into  $\hat{F}^{(\text{outlier})}$ .

In a similar manner, the non-outlier branch (Block 2b) is obtained by fitting  $h_m^{(\text{non-outlier})}$  to the negative gradient of the loss with respect to  $F^{(\text{non-outlier})}$

$$\begin{aligned} r_{i,m,t}^{(\text{non-outlier})} &= -\frac{\partial \mathcal{L}(y_{i,t}, F(\mathbf{x}_{i,t}))}{\partial \hat{F}^{(\text{non-outlier})}(\mathbf{x}_{i,t})} \\ &= -\frac{\partial \mathcal{L}(y_{i,t}, F(\mathbf{x}_{i,t}))}{\partial F(\mathbf{x}_{i,t})} \cdot \frac{\partial F(\mathbf{x}_{i,t})}{\partial \hat{F}^{(\text{non-outlier})}(\mathbf{x}_{i,t})}, \end{aligned} \quad (28)$$

which gives,

$$r_{i,m,t}^{(\text{non-outlier})} = -\frac{\partial \mathcal{L}(y_{i,t}, F(\mathbf{x}_{i,t}))}{\partial F(\mathbf{x}_{i,t})} \cdot (1 - \sigma(\theta_t)). \quad (29)$$

That is, the pseudo-residuals in this branch of the second block (Block 2b) are vectors pointing in the negative gradient of the loss with respect to  $\hat{F}^{(\text{non-outlier})}$ . Once a base learner  $h_m^{(\text{non-outlier})}$  has been fitted by minimizing Eq. (22), it is incorporated into  $\hat{F}^{(\text{non-outlier})}$ . These two steps, described to update  $\hat{F}^{(\text{non-outlier})}$  and  $\hat{F}^{(\text{outlier})}$ , are repeated for  $M_2$  iterations.

After generating each  $h_m^{(\text{outlier})}$  and each  $h_m^{(\text{non-outlier})}$  in Block 2, the parameter  $\theta_t$ , for each task is also updated. This dynamically adjusts the influence of each task  $t$  in the final ensemble prediction through a sigmoid-based weighting mechanism (See Eq. (15)).

Rather than explicitly labeling tasks as outliers or non-outliers, the model is *encouraged to learn* a soft partitioning, where the sigmoid activations of  $\theta_t$  tend towards—but do not always reach—extreme values close to 0 or 1. This soft activation enables flexible modulation of the contribution of each task to the outlier and non-outlier components. By doing so, the model can reduce the influence of anomalous outlier tasks, that may impair the **MTL** process, while emphasizing signals from more consistent tasks. As training progresses, negative gradients of the loss function  $\mathcal{L}$  with respect to parameter vector  $\theta$  guide this modulation, allowing the optimization process to adaptively infer and separate outlier tasks in a data-driven manner.

The update of  $\theta$  is done by taking a step of size  $\eta$  (*i.e.*, the learning rate) in the negative direction of the loss gradient with respect to  $\theta$ . That is,

$$\begin{aligned} -\frac{\partial \mathcal{L}}{\partial \theta} &= -\frac{\partial \mathcal{L}}{\partial F} \cdot \frac{\partial F}{\partial \theta} \\ &= -\sum_{t=1}^T \sum_{i=1}^{N^{(t)}} \frac{\partial \mathcal{L}(y_{i,t}, F(\mathbf{x}_{i,t}))}{\partial F(\mathbf{x}_{i,t})} \cdot \frac{\partial F(\mathbf{x}_{i,t})}{\partial \theta_t}, \end{aligned} \quad (30)$$

where,

$$\begin{aligned} -\frac{\partial F(\mathbf{x}_{i,t})}{\partial \theta_t} &= -\sigma(\theta_t) \cdot (1 - \sigma(\theta_t)) \cdot \hat{F}^{(\text{non-outlier})}(\mathbf{x}_{i,t}) \\ &\quad + \sigma(\theta_t) \cdot (1 - \sigma(\theta_t)) \cdot \hat{F}^{(\text{outlier})}(\mathbf{x}_{i,t}). \end{aligned} \quad (31)$$

Consequently, the negative gradient of the loss with respect to the parameter  $\theta_t$  (Eq. (30)) is computed as,

$$\begin{aligned} -\frac{\partial \mathcal{L}}{\partial \theta_t} &= \sum_{t=1}^T \sum_{i=1}^{N^{(t)}} r_{i,m,t}^{(\text{shared})} \cdot \sigma(\theta_t) \cdot (1 - \sigma(\theta_t)) \\ &\quad \cdot \left[ \hat{F}_t^{(\text{outlier})}(\mathbf{x}_{i,t}) - \hat{F}_t^{(\text{non-outlier})}(\mathbf{x}_{i,t}) \right]. \end{aligned} \quad (32)$$

**Block 3 - Task-Specific Fine-Tuning:** This block operates as a standard Single-Task (ST)-GB, initialized with the learned functions from previous blocks,  $\hat{F}^{(\text{shared})}$ ,  $\hat{F}^{(\text{outlier})}$  and  $\hat{F}^{(\text{non-outlier})}$ . Specifically, we simply update each  $\hat{F}_t^{(\text{task})}$  in Eq. (15). For this, each task independently fits  $h_m^{(\text{task})}(\mathbf{x}_i, r_{i,m,t}^{(\text{task})})$ , to the corresponding pseudo-residuals,

$$\begin{aligned} r_{i,m,t}^{(\text{task})} &= -\frac{\partial \mathcal{L}(y_{i,t}, F(\mathbf{x}_{i,t}))}{\partial \hat{F}^{(\text{task})}(\mathbf{x}_{i,t})} \\ &= -\frac{\partial \mathcal{L}(y_{i,t}, F(\mathbf{x}_{i,t}))}{\partial F(\mathbf{x}_{i,t})} \cdot \frac{\partial F(\mathbf{x}_{i,t})}{\partial \hat{F}^{(\text{task})}(\mathbf{x}_{i,t})} \\ &= -\frac{\partial \mathcal{L}(y_{i,t}, F(\mathbf{x}_{i,t}))}{\partial F(\mathbf{x}_{i,t})}. \end{aligned} \quad (33)$$

That is, the pseudo-residuals computed in Block 3 are vectors pointing in the negative gradient of the loss with respect to  $\hat{F}_t^{(\text{task})}$ , for each task  $t$ . Once a base learner  $h_m^{(\text{task})}$  has been fitted by minimizing Eq. (23), it is incorporated into  $\hat{F}_t^{(\text{task})}$ . This step is repeated for  $M_3$  iterations, for each task. The goal of this block is hence to allow each task to capture unique patterns not shared by previous blocks.

Note that the computation of the pseudo-residuals involves the evaluation of  $-\partial \mathcal{L}(y_{i,t}, F(\mathbf{x}_{i,t})) / \partial F(\mathbf{x}_{i,t})$ . Depending on the choice of the loss function for each problem type (*i.e.*, classification or regression), these gradients are computed differently. For classification, using the cross-entropy loss in Eq. (1), the gradients are defined as the difference between the true labels and predicted probabilities specified in Eq. (2). That is,

$$\frac{-\partial \mathcal{L}(y_{i,t}, F(\mathbf{x}_{i,t}))}{\partial F(\mathbf{x}_{i,t})} = y_{i,k} - P_{i,k}(\mathbf{x}_i). \quad (34)$$

In the case of regression, using the squared error loss defined in Eq. (3), the gradients are given by the difference between the true and predicted outputs,

$$\frac{-\partial \mathcal{L}(y_{i,t}, F(\mathbf{x}_{i,t}))}{\partial F(\mathbf{x}_{i,t})} = y_i - \hat{F}(\mathbf{x}_i). \quad (35)$$

The training procedure of **R-MTGB** is summarized in algorithm 1.

---

**Algorithm 1:** Robust-Multi-Task Gradient Boosting (**R-MTGB**) Training Procedure.

---

**Input :**  $\{\mathcal{D}_t\}_{t=1}^T, \mathcal{L}, M = M_1 + M_2 + M_3, \eta \in (0, 1], \theta \sim \mathcal{N}(\mu, \sigma^2)$   
**Output:**  $F(\mathbf{x})$

Initialize:  $\hat{F}_0^{\text{shared}} = \hat{F}_0^{\text{outlier}} = \hat{F}_0^{\text{non-outlier}} = \hat{F}_0^{\text{task}} = 0, \mathcal{D}_{\text{pool}} = \bigcup_{t=1}^T \mathcal{D}^{(t)}$

**Block 1: shared-Learning;**

**for**  $m = 1$  **to**  $M_1$  **do**

$\forall t, i : r_{i,m,t}^{(\text{shared})} \leftarrow \text{Eq. (25)};$   
 $h_m^{(\text{shared})} \leftarrow \text{fit}(\mathcal{D}_{\text{pool}}, r_m^{(\text{shared})});$   
 $\hat{F}_m^{(\text{shared})} \leftarrow \hat{F}_{m-1}^{(\text{shared})} + \eta h_m^{(\text{shared})}$

**Block 2: Outlier Partitioning;**

**for**  $m = (M_1 + 1)$  **to**  $(M_1 + M_2)$  **do**

$\forall t, i : r_{i,m,t}^{(\text{outlier})} \leftarrow \text{Eq. (27)}, r_{i,m,t}^{(\text{non-outlier})} \leftarrow \text{Eq. (29)};$   
 $h_m^{(\text{outlier})} \leftarrow \text{fit}(\mathcal{D}_{\text{pool}}, r_m^{(\text{outlier})}), \hat{F}_m^{(\text{outlier})} \leftarrow \hat{F}_{m-1}^{(\text{outlier})} + \eta h_m^{(\text{outlier})};$   
 $h_m^{(\text{non-outlier})} \leftarrow \text{fit}(\mathcal{D}_{\text{pool}}, r_m^{(\text{non-outlier})}), \hat{F}_m^{(\text{non-outlier})} \leftarrow \hat{F}_{m-1}^{(\text{non-outlier})} + \eta h_m^{(\text{non-outlier})};$   
 $\forall t : \theta_{m,t}^* \leftarrow \theta_{(m-1),t} - \eta \frac{\partial \mathcal{L}}{\partial \theta_{(m-1),t}}$  using Eq. (32);

**Block 3: Task-Specific Fine-Tuning;**

**for**  $m = (M_1 + M_2 + 1)$  **to**  $M$  **do**

**for**  $t = 1$  **to**  $T$  **do**  
 $\forall i : r_{i,m,t}^{(\text{task})} \leftarrow \text{Eq. (33)};$   
 $h_{m,t}^{(\text{task})} \leftarrow \text{fit}(\mathcal{D}_t, r_{m,t}^{(\text{task})});$   
 $\hat{F}_{m,t}^{(\text{task})} \leftarrow \hat{F}_{(m-1),t}^{(\text{task})} + \eta h_{m,t}^{(\text{task})}, (t)$

**return**  $\hat{F}^{(\text{shared})}(\mathbf{x}) + (1 - \sigma(\theta)) \cdot \hat{F}^{(\text{non-outlier})}(\mathbf{x}) + \sigma(\theta) \cdot \hat{F}^{(\text{outlier})}(\mathbf{x}) + \hat{F}^{(\text{task})}(\mathbf{x})$

---

### 3.5 Theoretical Analysis of Block 2

Block 2 guarantees that the contribution of each task to the empirical loss is bounded by a sigmoid weight, ensuring that outlier tasks cannot dominate the optimization. From Eq. (27), and Eq. (29), the pseudo-residuals are multiplied by  $\sigma(\theta)$  and  $(1 - \sigma(\theta))$ , so for every task  $t$  and sample  $i$ ,

$$|r_{i,m,t}^{(\text{outlier})}| \leq |r_{i,m,t}^{(\text{shared})}|, \quad |r_{i,m,t}^{(\text{non-outlier})}| \leq |r_{i,m,t}^{(\text{shared})}|. \quad (36)$$

To optimize the task-specific weights  $\theta_t$ , the model computes the negative gradient of the empirical risk with respect to  $\theta_t$  (see Eq. (32))

$$-\frac{\partial \mathcal{L}}{\partial \theta_t} = \sigma(\theta_t)(1 - \sigma(\theta_t)) S_t, \quad (37)$$

where,

$$S_t = \sum_{i=1}^{N_t} r_{i,m,t}^{(\text{shared})} \left( \hat{F}_t^{(\text{outlier})}(\mathbf{x}_{i,t}) - \hat{F}_t^{(\text{non-outlier})}(\mathbf{x}_{i,t}) \right). \quad (38)$$

Because  $\sigma(z) \in [0, 1]$  for all  $z$ , the product  $\sigma(z)(1 - \sigma(z))$  is always non-negative and is maximized at  $z = 0$ , with

$$0 \leq \sigma(z)(1 - \sigma(z)) \leq \frac{1}{4}, \quad \forall z \in \mathbb{R}.$$

Therefore, the Eq. (37) is bounded as,

$$\left| -\frac{\partial \mathcal{L}}{\partial \theta_t} \right| \leq \frac{1}{4} \sum_{i=1}^{N_t} |r_{i,m,t}^{(\text{shared})}| \left| \hat{F}_t^{(\text{outlier})}(\mathbf{x}_{i,t}) - \hat{F}_t^{(\text{non-outlier})}(\mathbf{x}_{i,t}) \right|. \quad (39)$$

This upper bound ensures stable updates and prevents extreme tasks from overwhelming the optimization.

**Proposition 1 (Task-wise direction of movement)** Because the sigmoid term  $\sigma(\theta_t)(1 - \sigma(\theta_t))$  is always non-negative, the direction of change for  $\theta_t$  during gradient descent depends solely on the sign of  $S_t$ ,

$$\text{sign}\left(-\frac{\partial \mathcal{L}}{\partial \theta_t}\right) = \text{sign}(S_t).$$

Thus, If  $S_t > 0$ , the loss decreases when  $\theta_t$  increases, making  $\sigma(\theta_t)$  larger. In this case, the task shifts its weight toward the *outlier* component. Conversely, if  $S_t < 0$ , the loss decreases when  $\theta_t$  decreases, making  $\sigma(\theta_t)$  smaller, and the task shifts its weight toward the *non-outlier* component. The sigmoid factor ensures smooth and bounded updates, preventing any single task from dominating the optimization. The exact direction (whether  $\sigma \rightarrow 0$  corresponds to the *non-outlier* or *outlier* component) depends on the initialization convention, but the mechanism consistently drives  $\theta_t$  toward the component that better reduces the loss for task  $t$ .

Regarding model complexity, the theoretical and empirical analyses presented in B indicate that the additional optimization introduced in Block 2 for task-specific parameters does not substantially increase computational cost compared to standard multi-task boosting. The model scales efficiently with the number of tasks while maintaining training stability.

## 4 Experiments and Results

To conduct the experiments, a combination of physical computing resources and developed code was utilized to support both the training and evaluation of the proposed and state-of-the-art models. The model was developed using Python (version 3.9), and scikit-learn (version 1.6)<sup>2</sup> [Pedregosa et al., 2011]. For transparency and reproducibility, the complete code-base, with the preprocessed dataset, has been made publicly accessible through the associated GitHub repository<sup>3</sup>.

To evaluate the proposed **R-MTGB** model, we conducted experiments alongside state-of-the-art models. These include: (1) a conventional multi-task **GB** model (**MTGB**) [Emami et al., 2023]; (2) **ST-GB**, a standard **GB** model trained independently for each task; (3) a data pooling approach where a standard **GB** model is trained on data from all tasks combined (**DP-GB**); and (4) a Task-as-Feature (**TaF-GB**), which is another data pooling approach in which the input data is augmented using an extra input feature with a one-hot encoding of the corresponding task identifier associated to each instance. The core implementations of **GB**, **TaF-GB**, and **DP-GB** are based on the standard **GB** framework proposed in Friedman [2001]. In real-world datasets, the models were trained and evaluated by randomly splitting the data into training and testing subsets using an 80:20 ratio. To ensure the reliability and robustness of the results, this process was repeated 100 times. For the synthetic datasets, 100 distinct train/test datasets were generated. For both real-world and synthetic datasets, we report the average performance across all tasks, followed by the average results computed over all repetitions.

We compare our proposed method, **R-MTGB**, primarily with **GB** and **MTGB**, as these methods represent the most relevant baselines to compare with. **GB** provides the natural point of reference since our method is an extension of this framework, and both **ST-GB** and pooled-task (**DP-GB**, **TaF-GB**) are variants that allow us to quantify the benefits of incorporating an **MTL** paradigm. **MTGB** is the closest existing approach, as it explicitly models shared and task-specific components within boosting. Nevertheless, **MTGB** lacks robustness to adversarial or outlier tasks. Direct comparison with **MTGB** therefore isolates the contribution of our outlier-aware design. By contrast, methods such as **TS-GB** [Chen et al., 2021] and FederBoost [Liu et al., 2024a] address orthogonal challenges—**TS-GB** focuses on modifying tree splitting criteria, and FederBoost targets privacy, preserving distributed learning—making them less appropriate for direct comparison.

To ensure consistent reporting and to facilitate fair comparisons of models performance, hyperparameters were optimized via 5-fold cross-validation within-training using a grid search. The grid search was configured to optimize Root Mean Squared Error (**RMSE**) for regression models and accuracy for classification models. This procedure was applied to both the synthetic (see Subsection 4.1) and the real-world datasets (see Subsection 4.2). Notably, all compared methods can be viewed as particular instances of **R-MTGB** framework, differentiated by the number of estimators to use in each different block. This generalization allows **R-MTGB** to flexibly encompass a wide range of model configurations under a unified framework. The ranges of hyperparameter values explored for each method are summarized in Table 2. Hyperparameters not listed in the table were set to their default values as defined in the **scikit-learn** library. Additionally, decision stumps were used as the base learner for all the studied models.

<sup>2</sup>[github.com/scikit-learn](https://github.com/scikit-learn)

<sup>3</sup>[github.com/GAA-UAM/R-MTGB](https://github.com/GAA-UAM/R-MTGB)

Table 2: Hyperparameter grid reporting the number of base learners considered for each method.

Model	No. of Base learners		
	1st Block	2nd Block	3rd Block
<b>R-MTGB</b>	[0, 20, 30, 50]	[20, 30, 50]	[0, 20, 30, 50, 100]
<b>MTGB</b>	[20, 30, 50]	–	[0, 20, 30, 50, 100]
<b>ST-GB</b>	–	–	[20, 30, 50, 100]
<b>DP-GB</b>	[20, 30, 50, 100]	–	–
<b>TAF-GB</b>	[20, 30, 50, 100]	–	–

#### 4.1 Synthetic Experiments

First, we conducted a series of experiments using synthetic data to validate the robustness of the developed **R-MTGB** model and to test our hypothesis prior to evaluation on real-world datasets. These synthetic datasets were generated using a combination of shared ( $\phi(\mathbf{x})$ ) and task-specific ( $\psi^{(t)}(\mathbf{x})$ ) functions. These functions are generated randomly using a framework based on Random Fourier Features [Rahimi and Recht, 2007]. Considering a multi-task dataset  $\mathcal{D}_t$  as defined in Eq. (4) and,

$$\mathbf{x}_{i,t} \sim \mathcal{U}([-1, 1]^d), \quad \forall i = 1, \dots, N^{(t)},$$

for a given input  $\mathbf{x} \in \mathbb{R}^d$ , the function output is generated with

$$\Psi(\mathbf{x}) = \sum_{i=1}^N \theta_i \sqrt{\frac{2\alpha}{D}} \cos \left( \mathbf{w}_i^\top \frac{\mathbf{x}}{d_x} + b_i \right), \quad (40)$$

where, each  $\mathbf{w}_i \sim \mathcal{N}(\mathbf{0}, \mathbf{I})$  denotes a random frequency vector, while  $b_i \sim \mathcal{U}(0, 2\pi)$  is a scalar phase shift. The random feature is weighted by  $\theta_i \sim \mathcal{N}(0, 1)$ , and the scaling hyperparameter is given by  $\alpha$ . The effective smoothness factor is defined as  $d_x = 0.5 \cdot d$ , where  $d$  is the input dimension. Finally,  $D$  denotes the number of random features, which is set to be equal to 500.

By using this generation process, the latent functions ( $\phi(\mathbf{x})$  and  $\psi^{(t)}(\mathbf{x})$ ) are approximately and independently sampled from a Gaussian process (GP) prior, as the Random Fourier Feature representation provides an explicit approximation of functions drawn from a stationary GP  $\Psi(\cdot)$ ,

$$\phi(\mathbf{x}) \sim \Psi(\mathbf{x}), \quad \psi^{(t)}(\mathbf{x}) \sim \Psi(\mathbf{x}).$$

(See Wilson et al. [2020] for further details).

For a set of  $T = T_{\text{non-out}} + T_{\text{out}}$  tasks,  $T_{\text{non-out}}$  *non-outlier* tasks can be generated by using a function defined as a combination of a common function and a task-specific function,

$$f_t^{(\text{non-out})}(\mathbf{x}) = w \cdot \phi(\mathbf{x}) + (1 - w) \cdot \psi^{(t)}(\mathbf{x}), \quad (41)$$

where,  $w$  is the combination weight, for  $t = 1, \dots, T_{\text{non-out}}$ . Similarly,  $T_{\text{out}}$  *outlier* tasks, on the other hand, are generated by replacing the shared function  $\phi$  with a different function  $\phi^{\text{out}}$  that is independently sampled,

$$f_t^{(\text{out})}(\mathbf{x}) = w \cdot \phi^{\text{out}}(\mathbf{x}) + (1 - w) \cdot \psi^{(t)}(\mathbf{x}), \quad (42)$$

for  $t = T_{\text{non-out}} + 1, \dots, T$ . For each instance  $\mathbf{x}_{i,t}$ , the target is generated by setting the continuous value  $y_{i,t}$  equal to the output of the corresponding function, *i.e.*,  $f_t^{(\text{non-out})}(\mathbf{x}_{i,t})$  or  $f_t^{(\text{out})}(\mathbf{x}_{i,t})$ , in regression. In binary classification, the class label is obtained by applying the sign function to the output of  $f_t^{(\text{non-out})}(\mathbf{x}_{i,t})$  or  $f_t^{(\text{out})}(\mathbf{x}_{i,t})$ .

An example of a generated toy dataset with one input and one output dimension, comprising seven non-outlier (common) tasks and one outlier task, is illustrated in Figure 1. The figure shows that the non-outlier tasks (tasks one to seven) cluster together and form a coherent band, indicating that they share an underlying functional structure. In contrast, task eight is distinguishable as an outlier. The data points of task eight diverge significantly from the smooth patterns observed in the other tasks. This distinction arises because task eight was generated using  $\phi^{\text{out}}$ , which differs from  $\phi$ , as described above.

Using the previously described techniques, we generated 100 random batches of a synthetic toy dataset, each initialized with a different random seed to ensure diversity, with a weighting parameter of  $w = 0.9$ . This guarantees

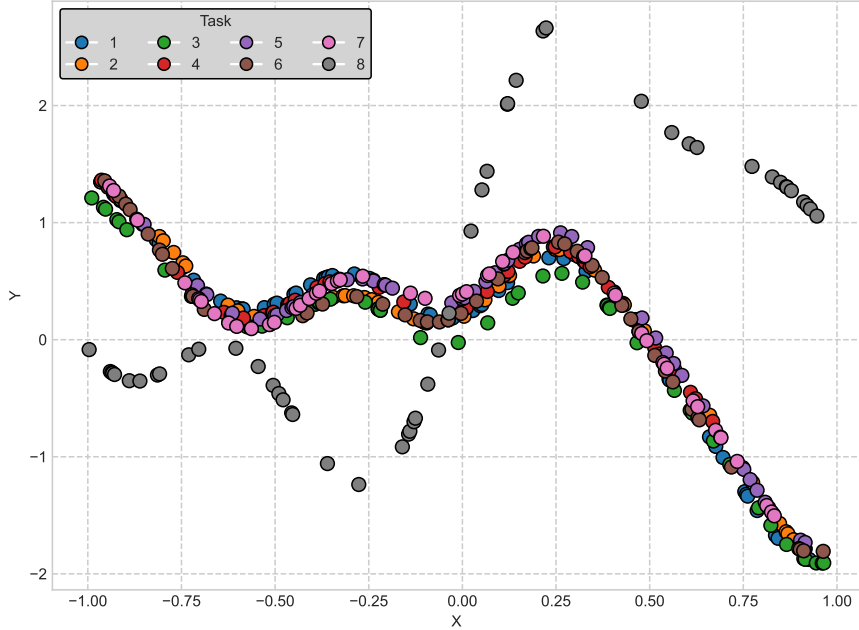


Figure 1: A visualization of the generated data points, comprising seven non-outlier (common) tasks (tasks 1 to 7) and one outlier task (task 8).

different functions for each task, for each batch. Each task consisted of 300 training instances and 1,000 test instances, distributed across five input features. To preserve class balance, we ensured that each class contained at least 10% of the total samples. Each batch included 10 tasks in total, two of which (last two tasks) were designated as outliers. We consider regression and binary classification settings. The generated datasets are publicly available on Mendeley Data<sup>4</sup>. For each batch of experiments, the models were trained using a fixed learning rate of one and a decision stump as the base learner. The number of base learners of each block was tuned using a 5-fold grid search cross-validation method on the training set. For this, we considered the hyperparameter grid defined in Table 2 for each method. The best set of hyperparameters found was then used for training the model. The performance of the evaluated models was measured using recall and accuracy for classification problem (Table 3), and Root Mean Squared Error (**RMSE**) and Mean Absolute Error (**MAE**) for regression problem (Table 4).

Table 3 shows the results obtained in the classification setting. The best-performing method in each metric is indicated in **bold**. The table shows that the introduced method, **R-MTGB**, achieves the highest test recall and accuracy among all evaluated methods, indicating strong generalization to unseen data.

Table 3: Average recall and accuracy scores with standard deviations, computed by first averaging across tasks and then over runs. Results are shown for each method on training and testing datasets, with best values per dataset in **bold**.

Model	Recall		Accuracy	
	Train	Test	Train	Test
<b>R-MTGB</b>	$0.882 \pm 0.090$	$\mathbf{0.829 \pm 0.108}$	$0.893 \pm 0.046$	$\mathbf{0.843 \pm 0.042}$
MTGB	$0.895 \pm 0.080$	$0.824 \pm 0.108$	$0.905 \pm 0.039$	$0.839 \pm 0.042$
DP-GB	$0.773 \pm 0.173$	$0.755 \pm 0.182$	$0.794 \pm 0.047$	$0.778 \pm 0.049$
ST-GB	$\mathbf{0.901 \pm 0.083}$	$0.819 \pm 0.114$	$\mathbf{0.911 \pm 0.039}$	$0.834 \pm 0.043$
TAF-GB	$0.801 \pm 0.144$	$0.782 \pm 0.154$	$0.816 \pm 0.042$	$0.800 \pm 0.045$

Regarding the regression setting, Table 4 shows the results obtained. Again, the best-performing methods per column are indicated in **bold**. We observe that the proposed method, **R-MTGB**, achieved the lowest **MAE** and **RMSE** on the test set, indicating the most accurate and robust regression performance on unseen data. As in the classification problem, **ST-GB** achieved slightly better performance on the training set, but exhibited higher test errors compared

<sup>4</sup>Multi-Task synthetic dataset

to **R-MTGB**. By contrast, the performance of **R-MTGB** remained consistent across training and testing for both problems, highlighting its ability to generalize effectively to unseen data. The performance gaps between the training and test results presented in Tables 3 and 4 for the different methods serve as indicators of each method’s regularization capability. The proposed **R-MTGB** method exhibits the smallest drop in performance between the training and test sets, demonstrating the most effective regularization among the evaluated methods.

Table 4: Average **MAE** and **RMSE** scores with standard deviations, computed by first averaging across tasks and then over runs. Results are shown for each method on training and testing datasets, with best values per dataset in bold.

Model	MAE		RMSE	
	Train	Test	Train	Test
<b>R-MTGB</b>	$0.309 \pm 0.041$	<b><math>0.332 \pm 0.043</math></b>	$0.397 \pm 0.053$	<b><math>0.426 \pm 0.055</math></b>
<b>MTGB</b>	$0.265 \pm 0.038$	$0.359 \pm 0.048$	$0.340 \pm 0.049$	$0.466 \pm 0.061$
<b>DP-GB</b>	$0.444 \pm 0.089$	$0.470 \pm 0.091$	$0.583 \pm 0.121$	$0.617 \pm 0.125$
<b>ST-GB</b>	<b><math>0.260 \pm 0.044</math></b>	$0.365 \pm 0.048$	<b><math>0.333 \pm 0.056</math></b>	$0.472 \pm 0.062$
<b>TAF-GB</b>	$0.387 \pm 0.062$	$0.412 \pm 0.065$	$0.504 \pm 0.081$	$0.537 \pm 0.085$

Figure 2 presents the average performance and standard deviation of each task-wise model, evaluated on the unseen portion of the same synthetic dataset described previously. The results are reported separately for classification tasks, using accuracy (left subplot), and for regression tasks, using **RMSE** (right subplot). Each model is depicted using a distinct color, with vertical lines around the means representing the standard deviation. From Figure 2, it can be observed that the proposed **R-MTGB** model outperforms both **MTGB** and **ST-GB** in all regression and most classification tasks. For classification (Figure 2, left subplot), **R-MTGB** model achieves the highest mean accuracy in the common tasks. For the outlier tasks, the studied models demonstrate comparable performance. Here, **R-MTGB** surpasses **MTGB**, whereas **ST-GB** performs negligibly better. Moreover, in the regression tasks (Figure 2, right subplot), **R-MTGB** outperforms all methods, in outlier and non-outlier tasks, demonstrating robustness and effective utilization of information from common tasks to achieve a strong performance across all tasks. Importantly, the absence of a weighting mechanism to identify outliers, causes **MTGB** approach to underperform in outlier tasks across both problem settings. Additional experiments, including the training and evaluation of a **DNN** model, are presented in A, showing that while **DNN** performed reasonably well on common tasks, it was less effective on outlier tasks, confirming the superior robustness and generalization of the proposed **R-MTGB** model.

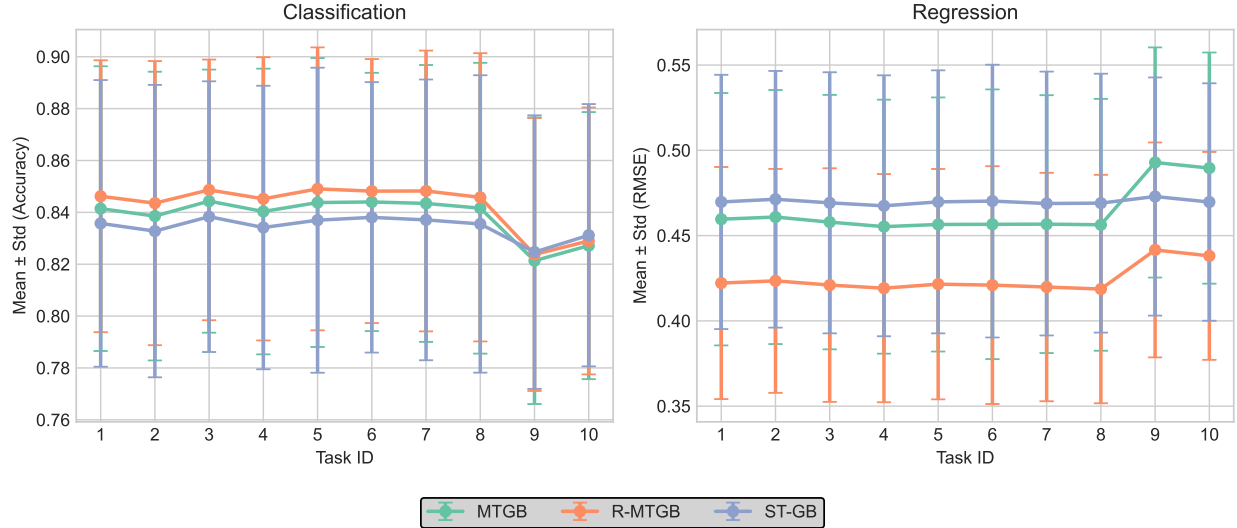


Figure 2: Average task-wise performance of the evaluated models over multiple runs shown separately for classification (left subplot) and regression (right subplot) tasks.

To assess the ability of the presented model to detect and identify the two defined outlier tasks, the mean and standard deviation of the learned  $\sigma(\theta)$  values by **R-MTGB** model are visualized in Figure 3 for regression and classification problems. The lines depict the mean values, while the shaded areas represent the corresponding standard deviations across multiple batches of experiments. The results for the classification setting are shown as a solid line with light

green shading, whereas the results for regression are depicted with a dashed line and light orange shading. The  $\sigma(\theta)$  values should split tasks into outliers and non-outliers, but it is not clear which extreme values will be assigned to outlier or non-outlier tasks due to the random initialization of the  $\theta$  values (See Subsection 3.5, *Proposition 1*, for further details). In any case, the results demonstrate that **R-MTGB** effectively identified outlier tasks by assigning them weights at the opposite extremes compared to non-outlier tasks. The small standard deviation observed across tasks, especially for the outlier tasks, further highlights the robustness of the designed parameter optimization.

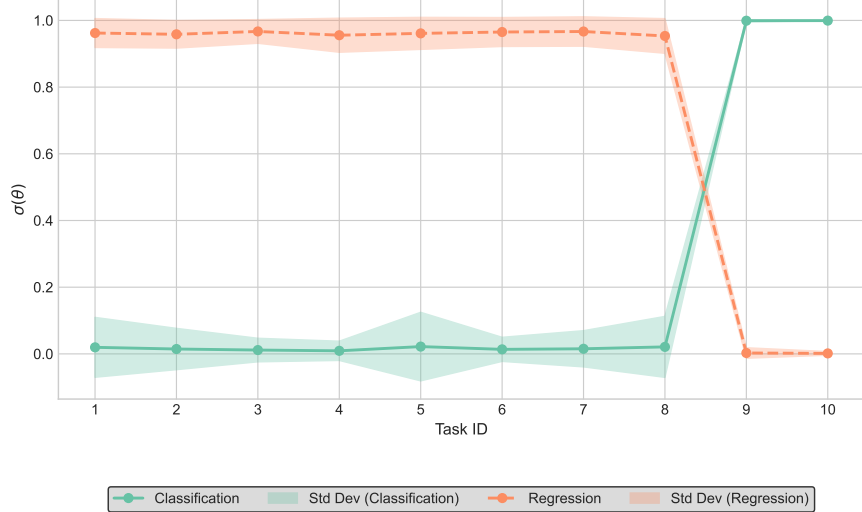


Figure 3: Mean and standard deviation of  $\sigma(\theta)$  for each task learned by **R-MTGB** model on the generated synthetic multi-task data. Values of  $\sigma(\theta)$  near 0 or 1 indicate task separation, with one extreme representing non-outlier tasks and the opposite extreme representing outlier tasks; the specific direction (0 = non-outlier vs. 1 = outlier, or vice versa) may depend on the problem.

#### 4.1.1 Key Benefits of RMTGB in Estimating Shared Functions

To further examine the effect of outlier tasks on shared function estimation in **MTL** models, we conducted an additional experiment using a one-dimensional toy dataset generated by Eq. (40). The dataset consisted of 10 tasks, including eight non-outlier tasks and two outlier tasks. Each task had 300 training instances, instantiated with both a shared component and a task-specific component (see Eq. (6) for further details). Figure 4 illustrates the generated training data across all tasks, with tasks one to eight categorized as non-outlier tasks, and tasks nine and ten designated as outlier tasks.

The purpose of this experiment is to see the effect of outlier tasks in the estimation of the common or shared function assumed by each method **MTGB** and **R-MTGB**. Specifically, it is expected that outlier tasks severely impair the estimation process in **MTGB**. Recall that **MTGB** assumes all tasks have a shared common function. To test this, we trained both **MTGB** and **R-MTGB** on this dataset using 150 base learners. Namely, 150 shared base learners for **MTGB** and 50 shared base learners (Block 1) and 100 outlier-aware base learners (Block 2), in **R-MTGB**. We did not consider any task-specific fitting, *i.e.*, the number of base learners in Block 3 is set equal to 0 in both **MTGB** and **R-MTGB**. We plotted the estimated functions obtained by each method across tasks. These functions should try to fit  $\phi(\mathbf{x})$  and  $\phi^{\text{out}}(\mathbf{x})$  in Eq. (41) and Eq. (42), respectively. Furthermore, we compare the corresponding estimates against the ground-truth function shared among tasks using in the data generation process.

Figure 5 shows the results for task one (non-outlier) and task ten (outlier) as representative examples, since the remaining tasks exhibit similar behavior. For each method, the figure shows performance in terms of **RMSE** estimation with respect to the actual function, *i.e.*,  $\phi(\mathbf{x})$  or  $\phi^{\text{out}}(\mathbf{x})$ . Overall generalization performance across all tasks is displayed in the figure title. We observe that the second block of the **R-MTGB** model enables it to correctly approximate the ground-truth shared function for both non-outlier task (left subplot) and outlier task (right subplot). By contrast, **MTGB** enforces a single shared function across all tasks, which becomes biased by the presence of outlier tasks, leading to poor fit for both components. In this experiment, the third block was not used (zero iterations), so the improvements stem solely from the combined effect of Block 1 (initial global shared-learning) and Block 2 (outlier-aware task partitioning). This behavior of **R-MTGB** prevents distortion of the shared representation, unlike in **MTGB**, ensuring that non-outlier tasks retain an accurate shared component, while outlier tasks are modeled jointly through

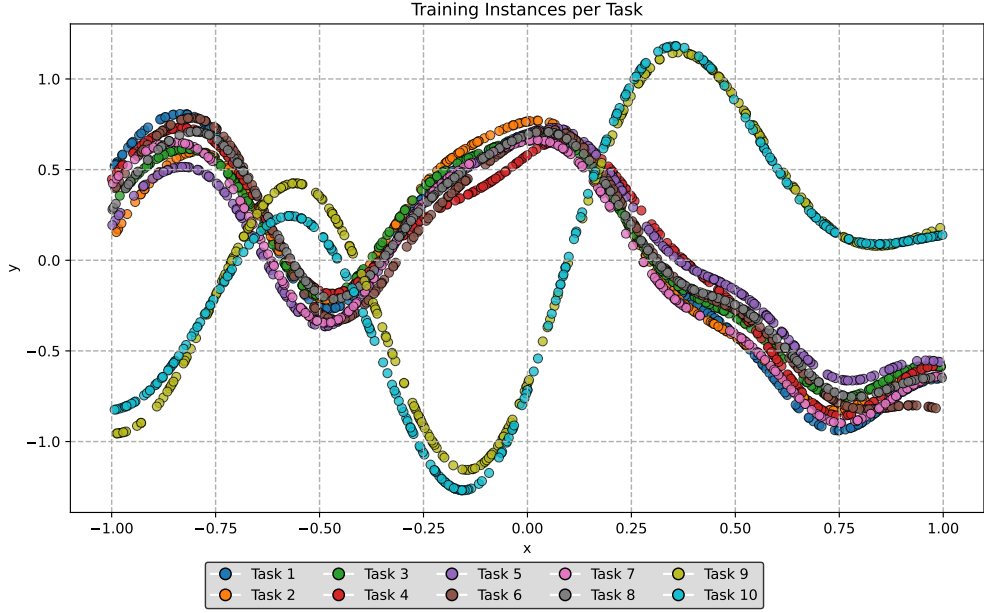


Figure 4: A visualization of the distribution of training data points, comprising eight non-outlier tasks (Tasks 1-8) and two outlier tasks (Tasks 9-10).

a separate shared component. As a result, **R-MTGB** achieves substantially lower overall error compared to **MTGB**, demonstrating its robustness in estimating shared functions under task heterogeneity. A better estimation of the shared component is expected to result in better generalization performance in real-world problems.

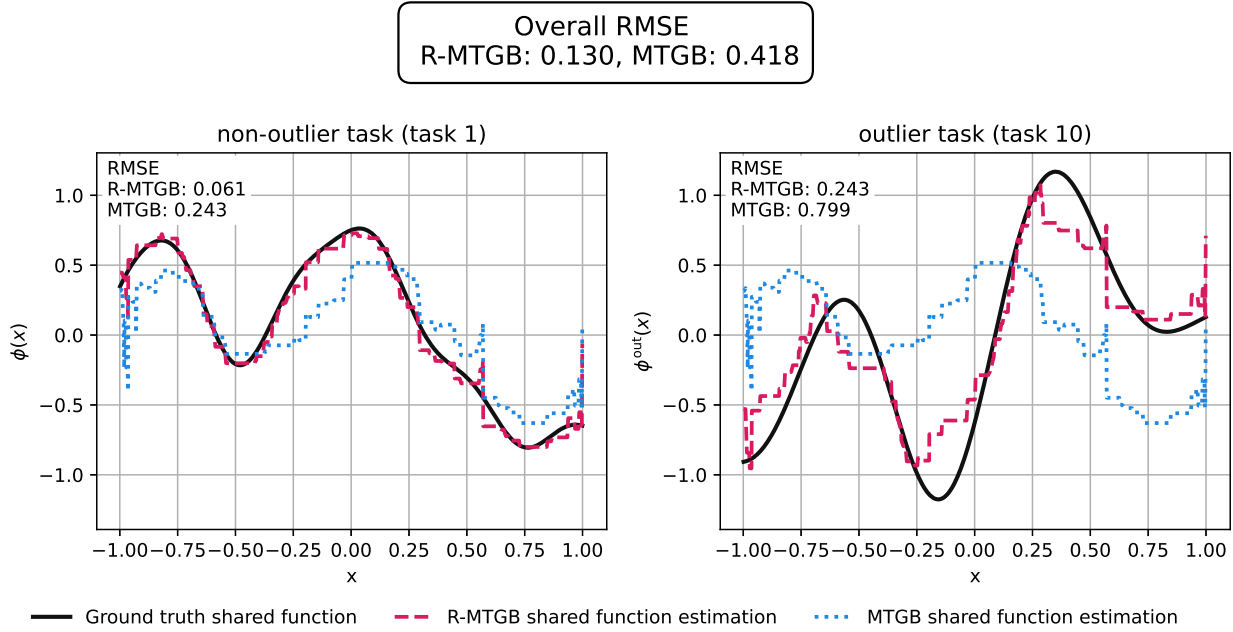


Figure 5: Comparison of shared function estimation results by **R-MTGB** and **MTGB** for a representative non-outlier task (left subplot) and a representative outlier task (right subplot).

## 4.2 Real-World Datasets Results

Table 5 presents a summary of the real-world datasets considered in our experiments, including their references, number of instances, features, tasks, and field of application. They are divided into two categories: classification and regression. Among the classification datasets, the *Avila* dataset is a multi-class problem with 12 classes, while the others are binary classification datasets. The distribution of instances across classes shows different levels of imbalance: in the *Adult* dataset, class 0 includes 37,155 instances and class 1 includes 11,687; in *Landmine*, there are 13,916 instances of class 0 and only 904 of class 1; and in *Bank Marketing*, class 0 has 39,922 instances compared to 5,289 of class 1. The *Avila* dataset is the most imbalanced, with class sizes ranging from just 10 instances (class 11) to 8,572 (class 0). In all the studied models, each sample contributes equally to the cross-entropy loss function (Eq. (1)), and the boosting process minimizes the average loss across all samples. Tasks are defined according to the natural structure of each dataset, such as copyist attribution (*Avila*), demographic groups (*Adult*), occupational categories (*Bank Marketing*), or sensor fields (*Landmine*). Similarly, the regression datasets are organized into tasks based on intrinsic attributes of the data, such as biological categories (*Abalone*), individual participants (*Parkinsons*), robotic joints, (*SARCOS*), school identifiers (*School*), or participant groups (*Computer*). These datasets have been widely adopted as benchmarks in recent MTL studies for both classification [Zhao et al., 2018, Oneto et al., 2019, Wang et al., 2021, Emami et al., 2023] and regression [Argyriou et al., 2007, 2008, Ciliberto et al., 2017, Gunduz, 2019, Wang et al., 2022b, Srinivasan et al., 2024] problems.

Table 5: Real-world datasets description.

Name	Instances	Attributes	Tasks	Field
<b>Classification</b>				
Avila [Stefano et al., 2018]	20,867	10	48	Handwriting Recognition
Adult [Becker and Kohavi, 1996]	48,842	14	7	Social Science
Bank Marketing [Moro et al., 2011]	45,211	16	12	Marketing
Landmine [Yilmaz et al., 2018]	14,820	9	29	Engineering
<b>Regression</b>				
Abalone [Nash et al., 1994]	4,177	8	3	Bioinformatics
Computer [Lenk et al., 1996]	3,800	13	190	Survey
Parkinsons [Tsanas and Little, 2009]	5,875	19	42	Biomedical
SARCOS [Jawanpuria et al., 2015]	342,531	21	7	Robotics
School [Bakker and Heskes, 2003]	15,362	10	139	Social Science

The experimental results of the evaluated models on real-world datasets (listed in Table 5) are summarized in Tables 6 through 9. All reported metrics are computed by first averaging across all tasks within each batch, and then calculating the mean and standard deviation over 100 batch runs. Note that each dataset contains a different number of tasks.

Specifically, Tables 6 and 7 present the average accuracy and unweighted mean recall on unseen test data for the classification datasets. Similarly, Tables 8 and 9 report the average **RMSE** and **MAE** on the test sets for the regression datasets. The best-performing results in each category are indicated in **boldface** per column.

The results in Table 6 clearly show that the proposed **R-MTGB** model consistently achieves the highest testing accuracy on all datasets, either matching or exceeding the performance of the competing methods. Notably, **R-MTGB** outperforms the other models on four out of five datasets and ties with **MTGB** on the *Landmine* dataset.

Table 6: Testing accuracy across models for each dataset, averaged first over tasks within each batch and then over runs. Mean and standard deviation are reported, with best values per dataset shown in bold.

Model	Adult (Gender)	Adult (Race)	Avila	Bank Marketing	Landmine
<b>R-MTGB</b>	<b><math>0.8493 \pm 0.0036</math></b>	<b><math>0.8487 \pm 0.0036</math></b>	<b><math>0.6190 \pm 0.0465</math></b>	<b><math>0.8947 \pm 0.0031</math></b>	<b><math>0.9428 \pm 0.0035</math></b>
<b>MTGB</b>	$0.8479 \pm 0.0036$	$0.8451 \pm 0.0036$	$0.6138 \pm 0.0503$	$0.8934 \pm 0.0030$	<b><math>0.9428 \pm 0.0035</math></b>
<b>DP-GB</b>	$0.8368 \pm 0.0046$	$0.8368 \pm 0.0046$	$0.4939 \pm 0.0095$	$0.8889 \pm 0.0029$	$0.9387 \pm 0.0035$
<b>ST-GB</b>	$0.8406 \pm 0.0036$	$0.8385 \pm 0.0036$	$0.6099 \pm 0.0605$	$0.8917 \pm 0.0030$	$0.9423 \pm 0.0035$
<b>TAF-GB</b>	$0.8368 \pm 0.0046$	$0.8368 \pm 0.0046$	$0.4970 \pm 0.0090$	$0.8889 \pm 0.0029$	$0.9387 \pm 0.0035$

As shown in Table 7, **R-MTGB** achieves the highest recall on three out of the five datasets: *Adult (Gender)*, *Adult (Race)*, and *Bank Marketing*, indicating strong overall performance across diverse classification tasks. **ST-GB** slightly outperforms **R-MTGB** on *Avila* and delivers the best result on *Landmine*, although the margin is small. In contrast, pooling-based approaches exhibit consistently lower recall and accuracy across all datasets, particularly on complex datasets such as *Avila*. Overall, these results further validate the effectiveness of **R-MTGB** in leveraging relational structure to enhance predictive performance across tasks.

An additional set of experimental results in terms of the F1 score is provided in A. These results show patterns consistent with the accuracy and recall findings: **R-MTGB** generally achieves the highest or near-highest F1 scores across most datasets, particularly in *Adult (Gender)*, *Adult (Race)*, and *Bank Marketing*, while **ST-GB** slightly outperforms it on *Avila* and *Landmine*. Overall, the F1-score analysis confirms that the proposed model maintains strong and balanced classification performance across heterogeneous tasks.

Table 7: Testing recall across models for each dataset, averaged first over tasks within each batch and then over runs. Mean and standard deviation are reported, with best values per dataset shown in bold.

Model	Adult (Gender)	Adult (Race)	Avila	Bank Marketing	Landmine
<b>R-MTGB</b>	<b><math>0.7256 \pm 0.0057</math></b>	<b><math>0.7248 \pm 0.0052</math></b>	$0.4360 \pm 0.0832$	<b><math>0.5892 \pm 0.0094</math></b>	$0.5478 \pm 0.0099$
<b>MTGB</b>	$0.7205 \pm 0.0051$	$0.7158 \pm 0.0080$	$0.4372 \pm 0.0853$	$0.5765 \pm 0.0099$	$0.5485 \pm 0.0100$
<b>DP-GB</b>	$0.6838 \pm 0.0099$	$0.6838 \pm 0.0099$	$0.1660 \pm 0.0083$	$0.5321 \pm 0.0037$	$0.5 \pm 0.0000$
<b>ST-GB</b>	$0.7049 \pm 0.0056$	$0.6931 \pm 0.0083$	<b><math>0.4534 \pm 0.0881</math></b>	$0.5552 \pm 0.0050$	<b><math>0.5518 \pm 0.0097</math></b>
<b>TAF-GB</b>	$0.6838 \pm 0.0099$	$0.6838 \pm 0.0099$	$0.1689 \pm 0.0069$	$0.5321 \pm 0.0037$	$0.5 \pm 0.0000$

Regarding the regression datasets and **RMSE** metric (Table 8), **R-MTGB** achieves the lowest test errors on nearly all datasets, demonstrating remarkable effectiveness, especially on datasets with structurally complex tasks (e.g., *SARCOS*). **ST-GB**, while not the top performer overall, achieves the best results on the *Parkinsons* dataset with a small margin over **R-MTGB**. pooling-based methods like **DP-GB** generally underperform, especially on more complex datasets like *Parkinsons* and *SARCOS*. In terms of **MAE** results (Table 9), **R-MTGB** again demonstrates consistent

Table 8: Testing **RMSE** across models for each dataset, averaged first over tasks within each batch and then over runs. Mean and standard deviation are reported, with best values per dataset shown in bold.

Model	Abalone	Computer	Parkinson	SARCOS	School
<b>R-MTGB</b>	<b><math>2.2660 \pm 0.0857</math></b>	<b><math>2.4632 \pm 0.0706</math></b>	$0.2868 \pm 0.0316$	<b><math>4.7031 \pm 0.0729</math></b>	<b><math>10.1313 \pm 0.1262</math></b>
<b>MTGB</b>	$2.2894 \pm 0.0866$	$2.4856 \pm 0.0473$	$0.3355 \pm 0.0243$	$4.8083 \pm 0.0336$	$10.1536 \pm 0.1222$
<b>DP-GB</b>	$2.3970 \pm 0.0935$	$2.4658 \pm 0.0478$	$8.8586 \pm 0.1373$	$18.3971 \pm 0.0669$	$10.4229 \pm 0.1176$
<b>ST-GB</b>	$2.3464 \pm 0.0889$	$2.7596 \pm 0.3516$	<b><math>0.2684 \pm 0.0274</math></b>	$4.9193 \pm 0.0340$	$10.2952 \pm 0.1366$
<b>TAF-GB</b>	$2.3830 \pm 0.0926$	$2.4668 \pm 0.0669$	$6.5588 \pm 0.0871$	$11.2658 \pm 0.0597$	$10.4152 \pm 0.1166$

superiority, achieving the lowest errors on the same datasets as those on **RMSE**, as shown in Table 8. **ST-GB** achieves the lowest **MAE** on *Parkinsons*, again with a minor difference compared to **R-MTGB**. As with the **RMSE** results, pooling-based methods such as **DP-GB** lag behind, particularly on complex datasets like *Parkinsons* and *SARCOS*. These results confirm the overall trend that **R-MTGB** offers a competitive and efficient alternative, striking a balance between accuracy and scalability by capturing relational information across tasks in a single model. In comparison

Table 9: Testing **MAE** across models for each dataset, averaged first over tasks within each batch and then over runs. Mean and standard deviation are reported, with best values per dataset shown in bold.

Model	Abalone	Computer	Parkinson	SARCOS	School
<b>R-MTGB</b>	<b><math>1.6073 \pm 0.0459</math></b>	<b><math>2.0208 \pm 0.0610</math></b>	$0.1315 \pm 0.0253$	<b><math>2.7366 \pm 0.0343</math></b>	<b><math>8.0048 \pm 0.1018</math></b>
<b>MTGB</b>	$1.6236 \pm 0.0468$	$2.0536 \pm 0.0437$	$0.1858 \pm 0.0154$	$2.7778 \pm 0.0156$	$8.0314 \pm 0.0955$
<b>DP-GB</b>	$1.7322 \pm 0.0502$	$2.0249 \pm 0.0432$	$7.3403 \pm 0.1180$	$12.6503 \pm 0.0469$	$8.2701 \pm 0.0975$
<b>ST-GB</b>	$1.6643 \pm 0.0481$	$2.1966 \pm 0.3169$	<b><math>0.1099 \pm 0.0082</math></b>	$2.7783 \pm 0.0154$	$8.1460 \pm 0.1083$
<b>TAF-GB</b>	$1.7110 \pm 0.0502$	$2.0430 \pm 0.0556$	$5.7127 \pm 0.0882$	$7.1316 \pm 0.0305$	$8.2696 \pm 0.0975$

with **MTGB** model, the proposed **R-MTGB** consistently outperforms it across all metrics, tasks, and datasets. This

demonstrates that the proposed approach effectively addresses the limitations of **MTGB** by incorporating a dynamic task weighting mechanism.

To systematically compare model performance across datasets (dataset-wise) and tasks (task-wise), as shown in Figures 6 and 7, we employ Demsar plots alongside the Nemenyi post-hoc test [Demšar, 2006], using a significance level of  $p = 0.05$ . A Demšar plot shows the average rank of each model across all evaluation scenarios. In the dataset-wise scenario, models are evaluated on each task, and performance is first averaged across all tasks and then averaged over 100 repetitions. In the task-wise scenario, the performance of each model on each task is averaged over 100 repetitions. In both scenarios, models are then ranked according to their averaged performance: in descending order for classification (where higher accuracy is better) and in ascending order for regression (where lower RMSE is better). The best-performing model receives rank one, the second-best rank two, and so on. The Demšar plot places each model along the horizontal axis according to this average rank, where models closer to the left have lower (better) ranks, indicating stronger overall performance. Finally, to determine whether differences between models are statistically significant, we apply the Nemenyi post-hoc test, which calculates Critical Distance (CD). If the average ranks of two models differ by more than the CD, their performance difference is considered statistically significant. In the corresponding plots, this is shown with horizontal bars: models connected by a bar are not significantly different in performance, and the calculated CDs are indicated above each subplot.

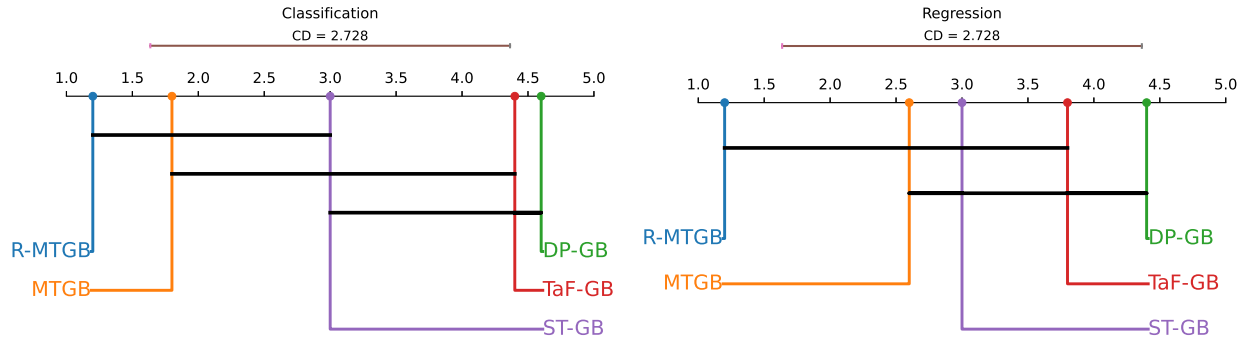


Figure 6: Demšar plots with the Nemenyi test ( $p = 0.05$ ) comparing model performance across datasets. Colors follow model rank order. The x-axis shows average ranks over 100 runs (lower is better). Horizontal bars mark no significant difference; the CD is shown at the top.

Our dataset-wise evaluation, as shown in Figure 6, covers ten datasets in total: five classification datasets (left subplot) and five regression datasets (right subplot). Figure 6 shows that **R-MTGB** model achieves the lowest (best) average rank for both classification and regression problems. Notably, **R-MTGB** maintains the best rank, followed by **MTGB**, with a larger margin for regression (Figure 6, right subplot). The consistently poor performance of **DP-GB** and **TaF-GB** across all scenarios in Figures 6 indicates that simple data aggregation can harm model effectiveness, likely due to the loss of task-specific distinctions. In contrast, the regularization mechanism in **R-MTGB** effectively leverages beneficial inter-task relationships while mitigating the negative effects of unrelated tasks, which is especially valuable in heterogeneous task environments.

For a more granular view, we perform a task-wise comparison by applying the same statistical procedure to individual tasks (Figure 7). For the ranking, the performance of each model on each task is averaged across all repetitions. This analysis includes 96 classification tasks measured by accuracy (left subplot) and 381 regression tasks, with performance measured by RMSE (right subplot). Figure 7, left subplot, shows that **R-MTGB** model achieves the lowest (best) average rank. Moreover, there is no statistically significant difference between the proposed model and **MTGB**; however, both methods outperform the remaining models, with the differences being statistically significant relative to the other evaluated approaches. In the regression tasks shown in the right subplot, the introduced model once again achieves the best (lowest) average rank. This improvement is statistically significant compared to all other evaluated methods, while the remaining models form a single group with no significant differences among them.

To evaluate the effectiveness of the proposed model in identifying outlier tasks, we analyzed the average optimized  $\sigma(\theta_t)$  value for each task  $t$  across the experimental datasets. These  $\sigma(\theta)$  values serve as task-specific outlier weights. After optimization, a value close to one indicates that the corresponding task is likely an outlier, whereas a value near zero suggests the task is likely a non-outlier or vice versa. Figure 8 shows the average learned  $\theta$  vector parameter by **R-MTGB** model, across 100 runs for each dataset (subplots) alongside the standard deviation (shaded region) for each task. To ensure consistent directionality across different experiment runs, each vector  $\sigma(\theta)$  is aligned with a reference vector (taken from the first run). Specifically, the first vector is stored as the reference. For each subsequent vector, the

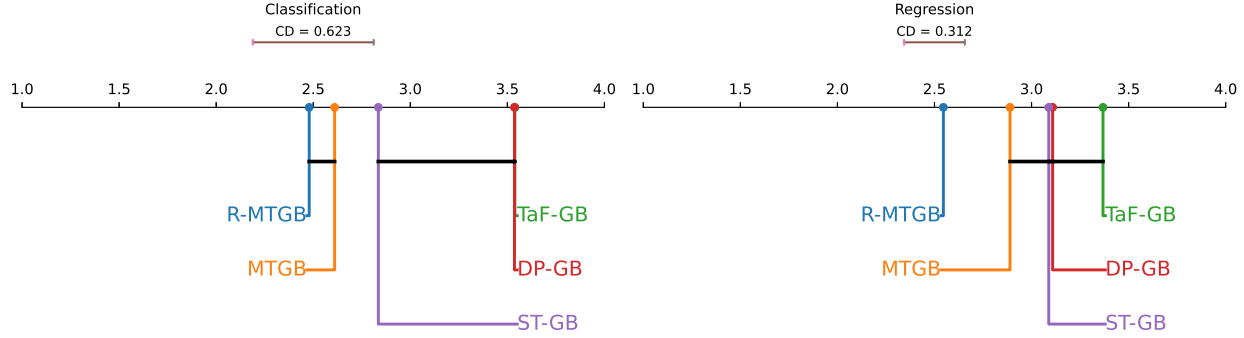


Figure 7: Demšar plots with the Nemenyi test ( $p = 0.05$ ) comparing model performance across tasks. Colors follow model rank order. The x-axis shows average ranks over 100 runs (lower is better). Horizontal bars mark no significant difference; the CD is shown at the top.

correlation with the reference is checked. If the correlation is negative (indicating opposite directionality) the vector is flipped by taking  $1 - \sigma(\theta)$ . This operation ensures that all vectors point in the same direction in the latent space, eliminating ambiguity due to symmetry. For datasets containing distinguishable or noisy tasks, such as *Avila*, *School*, and *Bank Marketing*, **R-MTGB** consistently assigned  $\sigma(\theta)$  values near the extremes, reflecting confident separation between non-outlier and outlier tasks. In contrast, *Adults* datasets exhibit minimal variation in  $\sigma(\theta)$ , which resulted in more uniform distributed  $\sigma(\theta)$  values. Moreover, the small standard deviation across tasks for complex datasets (e.g., *SARCOS*, *Avila*, and *Abalone*), indicates the robustness of the proposed model in identifying outlier tasks in various runs.

An additional experiment examining the training time of the studied models is presented in B. The empirical results show that, although **R-MTGB** incurs a moderately higher computational cost than **ST-GB** and pooling-based approaches due to its joint optimization and outlier detection mechanism, its training time remains comparable to that of standard **MTGB**. Across datasets, **R-MTGB** scales efficiently with increasing task numbers and dataset size, demonstrating stable and practical runtime performance despite its enhanced robustness.

## 5 Conclusions

This study introduced Robust-Multi-Task Gradient Boosting (**R-MTGB**), a principled methodology comprising three blocks designed to address task heterogeneity in Multi-Task Learning (**MTL**). **R-MTGB** sequentially integrates shared-level knowledge, outlier-aware task partitioning, and task-specific fine-tuning, to build a composite prediction model that effectively balances generalization and specialization. Its ensemble-based formulation employs a learned, task-dependent weighting mechanism to adaptively interpolate between outlier and non-outlier components, ensuring robust performance even in the presence of anomalous tasks. Notably, the model offers interpretability by revealing task-level outlier scores via the learned interpolation parameters, allowing for the diagnosis and visualization of tasks that significantly deviate from the shared structure.

Comprehensive experiments conducted on both synthetic and real-world datasets demonstrate the ability of the proposed model to generalize across tasks, maintain high predictive accuracy for each individual task, and robustly identify anomalous tasks. The results indicate that **R-MTGB** outperforms Multi-Task Gradient Boosting (**MTGB**), Single-Task (**ST**) learning, and Data Pooling (**DP**) approaches, including augmented data pooling with task-specific information. Our experiments show that the proposed method offers advantages in both settings, though they are more pronounced in the regression setting than in classification problems. These advantages hold across varying degrees of task heterogeneity, underscoring the robustness and adaptability of the developed **MTL** framework.

Finally, the proposed three-block structure, along with the learnable parameter, is both empirically validated and theoretically analyzed and bounded.

Future work could extend **R-MTGB** to jointly learn all blocks, rather than sequentially, which may improve optimality by allowing the model to reconsider the inclusion or exclusion of base learners across blocks. Currently, once base learners are incorporated in the first block, they cannot be removed even if they prove unnecessary in later blocks. Additionally, the method could be extended to handle multiple task groups beyond the current outlier/non-outlier distinction, enabling it to automatically identify clusters of related tasks while isolating unrelated ones.

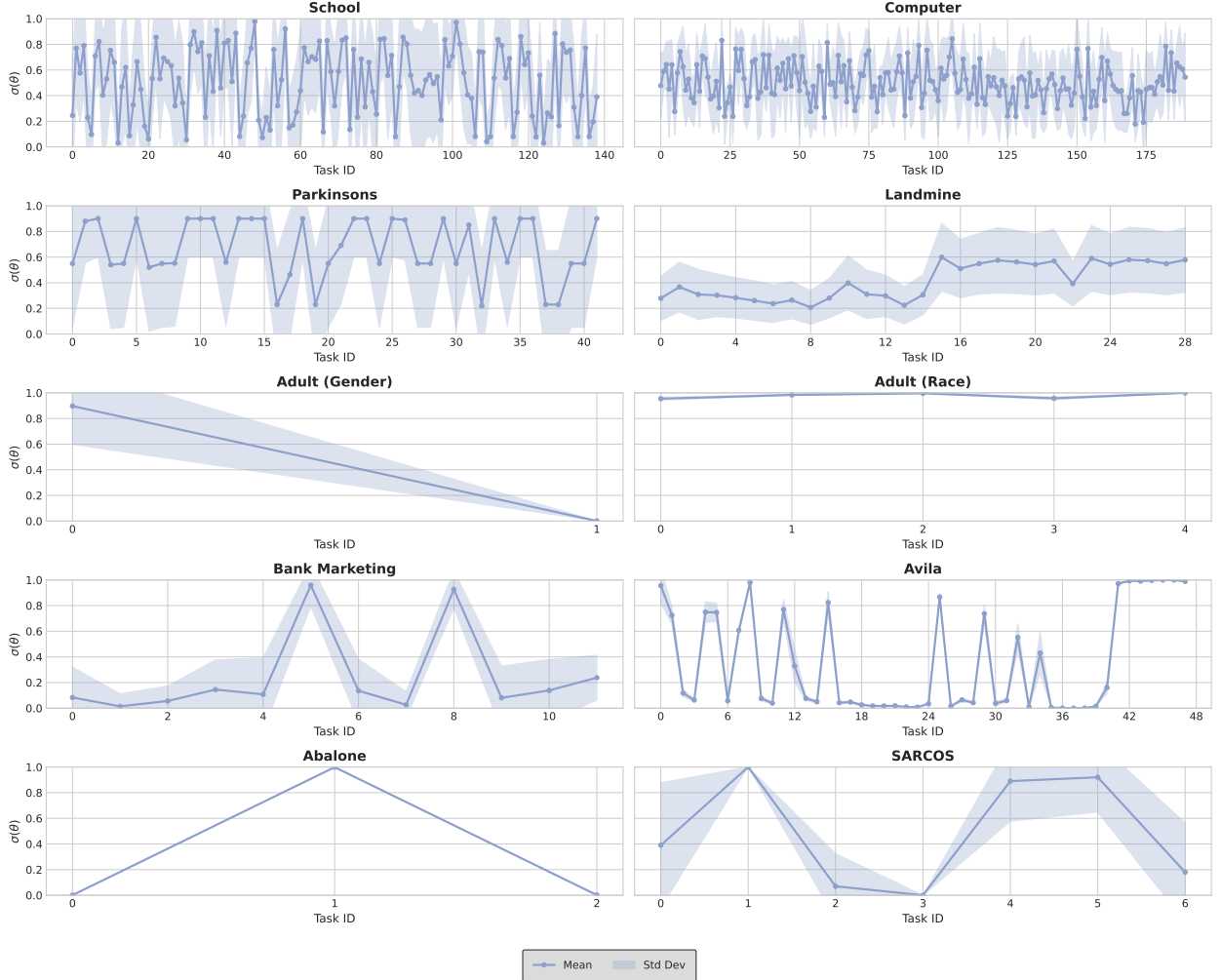


Figure 8: Mean and standard deviation of the learned  $\sigma(\theta)$  values across multiple runs for each task, shown separately for each dataset in the corresponding subplots. Values of  $\sigma(\theta)$  close to 0 or 1 indicate a clear separation between non-outlier and outlier tasks, with the specific direction depending on initialization and alignment. The shaded areas represent the variability across runs. These results demonstrate that R-MTGB consistently identifies and distinguishes outlier tasks from non-outlier tasks, even in heterogeneous and noisy datasets.

## Declaration of Interests

The authors declare that there are no competing financial interests or personal relationships that could have potentially biased the research, experiments, or the conclusions presented in this manuscript.

## Acknowledgments

The authors acknowledge financial support from the project PID2022-139856NB-I00, funded by MCIN/AEI/10.13039/501100011033/FEDER, UE; from project IDEA-CM (TEC-2024/COM-89), funded by the Autonomous Community of Madrid; and from the ELLIS Unit Madrid. The authors also acknowledge computational support from the Centro de Computación Científica-Universidad Autónoma de Madrid (CCC-UAM).

## Data and Code Availability

The datasets utilized in this study were obtained from their respective publicly cited references. Both these datasets and the public source developed code for the proposed model are accessible at [github.com/GAA-UAM/R-MTGB](https://github.com/GAA-UAM/R-MTGB).

## A Additional Experiments

In this appendix, we report additional experiments to further enrich the evaluation of the studied models. Table 10 presents the testing macro F1 scores across datasets and models. For each run, the F1 score was computed using the *macro* averaging scheme, which calculates the F1 score independently for each class and then takes the unweighted mean.

Scores were first averaged over tasks within each batch and then across repetitions, with both the mean and standard deviation reported in the Table 10. As shown in Table 10, R-MTGB achieves the highest or near-highest macro F1 scores on most datasets, notably *Adult (Gender)*, *Adult (Race)*, and *Bank Marketing*. For the *Avila* and *Landmine* datasets, ST-GB baseline slightly outperforms R-MTGB.

Table 10: Testing F1 score across models for each dataset, averaged first over tasks within each batch and then over runs. Mean and standard deviation are reported, with best values per dataset shown in bold.

Model	Adult (Gender)	Adult (Race)	Avila	Bank Marketing	Landmine
<b>R-MTGB</b>	<b><math>0.7574 \pm 0.0058</math></b>	<b><math>0.7565 \pm 0.0054</math></b>	$0.4595 \pm 0.0969$	<b><math>0.6198 \pm 0.0126</math></b>	$0.5713 \pm 0.0163$
MTGB	$0.7531 \pm 0.0055$	$0.7477 \pm 0.0074$	$0.4605 \pm 0.1014$	$0.6024 \pm 0.0137$	$0.5725 \pm 0.0165$
DP-GB	$0.7173 \pm 0.0107$	$0.7173 \pm 0.0107$	$0.1442 \pm 0.0062$	$0.5317 \pm 0.0067$	$0.4842 \pm 0.0009$
ST-GB	$0.7369 \pm 0.0060$	$0.7263 \pm 0.0080$	<b><math>0.4629 \pm 0.1087</math></b>	$0.5711 \pm 0.0082$	<b><math>0.5772 \pm 0.0155</math></b>
TAF-GB	$0.7173 \pm 0.0107$	$0.7173 \pm 0.0107$	$0.1466 \pm 0.0058$	$0.5317 \pm 0.0067$	$0.4842 \pm 0.0009$

To extend the experiment to a deep learning framework, we incorporated a DNN model into an additional batch of experiments. The DNN was trained on the pooled data from all tasks, allowing the model to learn a shared representation that captures general patterns across. This configuration serves as a deep-learning benchmark that leverages cross-task information to enhance representation learning and allows a direct empirical comparison with the boosting-based MTL models.

The trained DNN architecture consists of three fully connected hidden layers with 100 neurons each, using the Rectified Linear Unit (ReLU) as the activation function. Training was performed for a maximum of 100 epochs with an L2 regularization parameter of 0.0001. A grid search over the learning rate initialization values [0.001, 0.01, 0.1] was conducted for hyperparameter tuning using 5-fold cross-validation. All input features were standardized through a preprocessing pipeline, and model training was conducted using the scikit-learn library.

The DNN was trained on the same 100 distinct synthetic train/test datasets described in Subsection 4.1. summarized in Tables 11 and 12, provides a complementary benchmark to the boosting-based MTL models presented earlier (See Subsection 4.1).

As shown in Table 11, DNN attains competitive classification performance. Its test accuracy and recall are close to those of R-MTGB, (see Table 3), placing R-MTGB as the top-performing model in terms of accuracy and the second-best in recall, with an insignificant difference between the two.

Table 11: Average recall and accuracy scores of DNN with standard deviations, computed by first averaging across tasks and then over runs.

Model	Recall		Accuracy	
	Train	Test	Train	Test
DNN	$0.871 \pm 0.117$	$0.830 \pm 0.118$	$0.880 \pm 0.043$	$0.841 \pm 0.034$

According to Table 12 and Table 4, R-MTGB achieves the best generalization performance with the lowest test MAE and RMSE. The performance gap between DNN and the proposed model highlights the advantage of R-MTGB in capturing inter-task structure and mitigating the impact of outlier tasks, confirming its superior robustness in heterogeneous multi-task settings.

Table 12: Average **MAE** and **RMSE** scores of **DNN** with standard deviations, computed by first averaging across tasks and then over runs.

Model	MAE		RMSE	
	Train	Test	Train	Test
<b>DNN</b>	$0.323 \pm 0.113$	$0.380 \pm 0.105$	$0.458 \pm 0.145$	$0.546 \pm 0.141$

To further examine the performance of **DNN** across tasks, Figure 9 presents the average **DNN** results per task across all repetitions—analogous to Figure 2. Specifically, the left subplot of Figure 9 illustrates classification accuracy, while the right subplot displays regression performance measured by **RMSE**. Comparing Figures 9 and 2 (left subplots), we observe that **DNN** achieves better results on non-outlier tasks (tasks 1 to 8) relative to the proposed models, but struggles with outlier tasks. This is particularly evident in the last two tasks (Tasks 9 and 10), where accuracy drops significantly.

For regression (right subplots of Figure 9 and Figure 2), **DNN** achieves comparable performance to the proposed model on non-outlier tasks, but again fails to generalize to outlier tasks, resulting in large errors and a substantial performance gap relative to the proposed approach.

Given the performance of **DNN** on the synthetic datasets, we omit experiments using **DNN** on real-world datasets, as the complex synthetic setup already provides a sufficient basis for comparison.

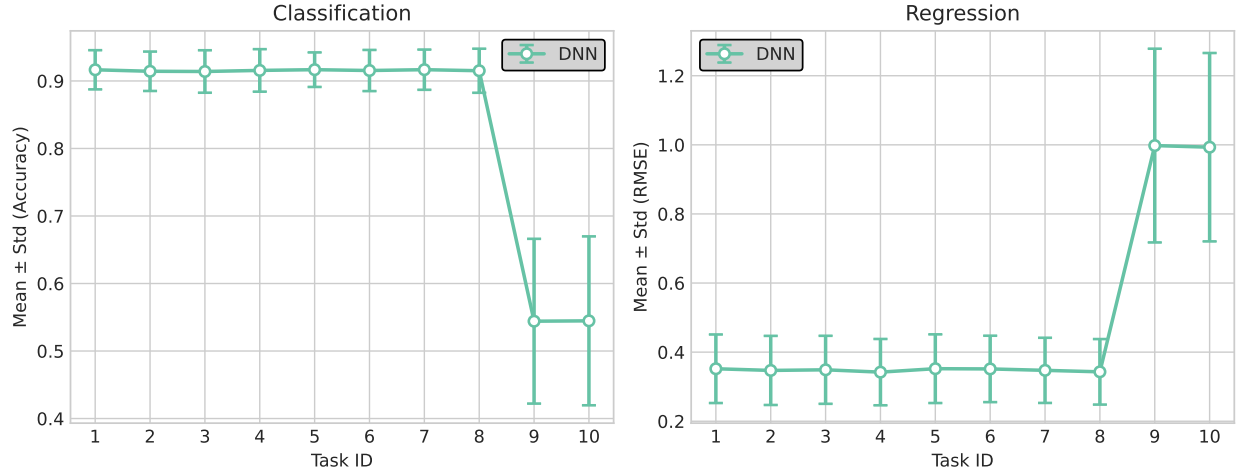


Figure 9: Average task-wise performance of the **DNN** over multiple runs shown separately for classification (left subplot) and regression (right subplot) tasks.

## B Complexity and Training Efficiency

In this section, we provide both theoretical and empirical analyses of the computational complexity of the models studied in this paper. For the theoretical analysis, we employ Big  $\mathcal{O}$  notation to describe the time complexity of each model.

Let  $N = \sum_{t=1}^T N_t$  be the pooled number of samples,  $d$  the number of features, and  $\text{Tree}(n, d)$  the cost of fitting one decision stump on  $n$  samples with  $d$  features. For stumps we approximate  $\text{Tree}(n, d) = \mathcal{O}(nd \log n)$ . We additionally assume that all tasks have similar size, i.e.  $N_t \approx N/T$ .

- **ST-GB**: trains one model per task with  $M_3$  trees each:

$$\begin{aligned}
 \mathcal{O}\left(\sum_{t=1}^T M_3 \text{Tree}(N_t, d)\right) &\approx \mathcal{O}\left(TM_3 \text{Tree}(N/T, d)\right) \\
 &= \mathcal{O}\left(M_3 N d \log(N/T)\right).
 \end{aligned}$$

- **MTGB (shared + per-task):** Block 1 fits one multi-output stump per iteration on pooled data (not one per task).

$$\begin{aligned} & \mathcal{O}\left(M_1 \text{Tree}(N, d) + TM_3 \text{Tree}(N/T, d)\right) \\ & \approx \mathcal{O}\left(M_1 Nd \log N + M_3 Nd \log(N/T)\right). \end{aligned}$$

- **R-MTGB:** Block 2 adds two pooled trees per iteration. Updating  $\theta_t$  costs only  $c_\theta(N_t) = \mathcal{O}(N_t)$ , negligible relative to  $\text{Tree}(N, d)$ .

$$\begin{aligned} \text{Block 2: } & \mathcal{O}(2M_2 \text{Tree}(N, d)) \\ & = \mathcal{O}(2M_2 Nd \log N). \end{aligned}$$

Combining the three blocks yields

$$\begin{aligned} & \mathcal{O}\left(M_1 \text{Tree}(N, d) + 2M_2 \text{Tree}(N, d) + TM_3 \text{Tree}(N/T, d)\right) \\ & \approx \mathcal{O}\left((M_1 + 2M_2) Nd \log N + M_3 Nd \log(N/T)\right). \end{aligned}$$

Under the equal-task-size assumption and stump model, all methods exhibit the same *highest-order complexity*, differing only in constant factors and in how the iterations  $M_1, M_2, M_3$  are distributed across blocks.

For the empirical analysis, all models were trained using their default hyperparameter settings, as described in Section 4. The number of estimators per block and per model was tuned using the grid specified in Table 2. Two representative datasets (*Adult (Gender)*) for classification and *Parkinsons* for regression) were selected for the experiments. Each training procedure was repeated independently five times, and the mean and standard deviation of the results are reported in Table 13, with the lowest elapsed time highlighted in **bold**. Elapsed times were measured on a Linux-based system using CPU processing time. The experiments were conducted on a machine equipped with two Intel(R) Xeon(R) E5-2620 v3 CPUs (2.40 GHz, 6 cores per socket, 24 threads in total) and 64 GB of RAM. The reported times correspond to the sum of system CPU time consumed by each training process, excluding any sleep or idle time. The elapsed training time was recorded in seconds by comparing timestamps before and after the training phase.

Table 13: Average training time for each method, in seconds, including estimating the hyperparameters using the inner CV procedure and fitting the final model. Lowest times are highlighted in **bold**.

Model	Adult (Gender)	Parkinson
<b>R-MTGB</b>	$12.9838014 \pm 0.8103452$	$4.0310959 \pm 0.1997661$
<b>MTGB</b>	$8.1746369 \pm 0.5158048$	$3.2083791 \pm 0.1308600$
<b>DP-GB</b>	$6.1319405 \pm 0.3305553$	<b><math>0.9071499 \pm 0.0655788</math></b>
<b>ST-GB</b>	$6.4622585 \pm 0.4245966$	$2.9695122 \pm 0.1109322$
<b>TAF-GB</b>	<b><math>5.7476897 \pm 0.2548860</math></b>	$1.0148046 \pm 0.0911100$

Based on the measured training times reported in Table 13, models that rely on pooled data are the fastest to train. **ST-GB** follows closely, remaining computationally cheaper than the multi-task approaches. In contrast, **MTGB** requires more time. Among all methods, **R-MTGB** exhibits the highest training time. Its three-block architecture, together with the larger number of hyperparameters that must be tuned, makes it more computationally demanding than the alternatives. A similar, though smaller, effect is observed for **MTGB**, whose additional hyperparameter increases its training cost relative to pooling-based and single-task models. Despite this, the difference in runtime between **R-MTGB** and **MTGB** remains moderate, indicating that the robustness gains provided by **R-MTGB** are achieved with only a reasonable computational overhead.

## References

Ahmed Agiza, Marina Neseem, and Sherief Reda. MTLoRA: Low-Rank Adaptation Approach for Efficient Multi-Task Learning. In *Proceedings of the IEEE/CVF Conference on Computer Vision and Pattern Recognition (CVPR)*, pages 16196–16205, 2024.

Rie Kubota Ando, Tong Zhang, and Peter Bartlett. A framework for learning predictive structures from multiple tasks and unlabeled data. *Journal of machine learning research*, 6(11), 2005.

Raquel Aoki, Frederick Tung, and Gabriel L. Oliveira. Heterogeneous Multi-Task Learning With Expert Diversity. *IEEE/ACM Transactions on Computational Biology and Bioinformatics*, 19(6):3093–3102, 2022.

Andreas Argyriou, Massimiliano Pontil, Yiming Ying, and Charles Micchelli. A Spectral Regularization Framework for Multi-Task Structure Learning. In *Advances in Neural Information Processing Systems*, volume 20. Curran Associates, Inc., 2007.

Andreas Argyriou, Theodoros Evgeniou, and Massimiliano Pontil. Convex multi-task feature learning. *Machine Learning*, 73(3):243–272, 2008.

Bart Bakker and Tom Heskes. Task clustering and gating for bayesian multitask learning. *Journal of Machine Learning Research*, 4:83–99, 2003.

Barry Becker and Ronny Kohavi. Adult. <https://archive.ics.uci.edu>, 1996.

Alexis Bellot and Mihaela van der Schaar. Multitask Boosting for Survival Analysis with Competing Risks. In *Advances in Neural Information Processing Systems*, volume 31. Curran Associates, Inc., 2018.

Candice Bentéjac, Anna Csörgő, and Gonzalo Martínez-Muñoz. A comparative analysis of gradient boosting algorithms. *Artificial Intelligence Review*, 54(3):1937–1967, 2021.

Vadim Borisov, Tobias Leemann, Kathrin Seßler, Johannes Haug, Martin Pawelczyk, and Gjergji Kasneci. Deep Neural Networks and Tabular Data: A Survey. *IEEE Transactions on Neural Networks and Learning Systems*, 35(6):7499–7519, 2024.

Rich Caruana. Multitask Learning. *Machine Learning*, 28(1):41–75, 1997.

Olivier Chapelle, Pannagadatta Shivaswamy, Srinivas Vadrevu, Kilian Weinberger, Ya Zhang, and Belle Tseng. Boosted multi-task learning. *Machine Learning*, 85(1-2):149–173, 2011.

Jianhui Chen, Jiayu Zhou, and Jieping Ye. Integrating low-rank and group-sparse structures for robust multi-task learning. In *Proceedings of the 17th ACM SIGKDD International Conference on Knowledge Discovery and Data Mining*, pages 42–50. Association for Computing Machinery, 2011.

Mingcheng Chen, Zhenghui Wang, Zhiyun Zhao, Weinan Zhang, Xiawei Guo, Jian Shen, Yanru Qu, Jielu Lu, Min Xu, Yu Xu, Tiange Wang, Mian Li, Weiwei Tu, Yong Yu, Yufang Bi, Weiqing Wang, and Guang Ning. Task-wise Split Gradient Boosting Trees for Multi-center Diabetes Prediction. In *Proceedings of the 27th ACM SIGKDD Conference on Knowledge Discovery & Data Mining*, pages 2663–2673, 2021.

Shijie Chen, Yu Zhang, and Qiang Yang. Multi-Task Learning in Natural Language Processing: An Overview. *ACM Comput. Surv.*, 56(12), 2024.

Tianqi Chen and Carlos Guestrin. XGBoost: A Scalable Tree Boosting System. In *Proceedings of the 22nd ACM SIGKDD International Conference on Knowledge Discovery and Data Mining*, pages 785–794. Association for Computing Machinery, 2016.

Carlo Ciliberto, Alessandro Rudi, Lorenzo Rosasco, and Massimiliano Pontil. Consistent Multitask Learning with Nonlinear Output Relations. In *Advances in Neural Information Processing Systems*, volume 30. Curran Associates, Inc., 2017.

Koby Crammer and Yishay Mansour. Learning Multiple Tasks using Shared Hypotheses. In *Advances in Neural Information Processing Systems*, volume 25. Curran Associates, Inc., 2012.

Pádraig Cunningham, Matthieu Cord, and Sarah Jane Delany. *Supervised Learning*, pages 21–49. Springer Berlin Heidelberg, 2008.

Janez Demšar. Statistical comparisons of classifiers over multiple data sets. *The Journal of Machine Learning Research*, 7:1–30, 2006.

Seyedsaman Emami and Gonzalo Martínez-Muñoz. Condensed-gradient boosting. *International Journal of Machine Learning and Cybernetics*, 16(1):687–701, 2025.

Seyedsaman Emami, Carlos Ruiz Pastor, and Gonzalo Martínez-Muñoz. Multi-Task Gradient Boosting. In *Hybrid Artificial Intelligent Systems*, pages 97–107. Springer International Publishing, 2023.

Theodoros Evgeniou and Massimiliano Pontil. Regularized multi-task learning. In *Proceedings of the Tenth ACM SIGKDD International Conference on Knowledge Discovery and Data Mining*, pages 109–117. Association for Computing Machinery, 2004.

Theodoros Evgeniou, Charles A Micchelli, Massimiliano Pontil, and John Shawe-Taylor. Learning multiple tasks with kernel methods. *Journal of machine learning research*, 6(4), 2005.

Maxime Fontana, Michael Spratling, and Miaojing Shi. When Multitask Learning Meets Partial Supervision: A Computer Vision Review. *Proceedings of the IEEE*, 112(6):516–543, 2024.

Jerome H. Friedman. Greedy Function Approximation: A Gradient Boosting Machine. *The Annals of Statistics*, 29(5):1189–1232, 2001.

Pinghua Gong, Jieping Ye, and Changshui Zhang. Robust multi-task feature learning. In *Proceedings of the 18th ACM SIGKDD international conference on Knowledge discovery and data mining*, pages 895–903, 2012.

Leo Grinsztajn, Edouard Oyallon, and Gael Varoquaux. Why do tree-based models still outperform deep learning on typical tabular data? In *Advances in Neural Information Processing Systems*, volume 35, pages 507–520. Curran Associates, Inc., 2022.

Nuwan Gunasekara, Bernhard Pfahringer, Heitor Gomes, and Albert Bifet. Gradient boosted trees for evolving data streams. *Machine Learning*, 113(5):3325–3352, 2024.

Hakan Gunduz. Deep Learning-Based Parkinson’s Disease Classification Using Vocal Feature Sets. *IEEE Access*, 7: 115540–115551, 2019.

Lei Han and Yu Zhang. Learning Tree Structure in Multi-Task Learning. In *Proceedings of the 21th ACM SIGKDD International Conference on Knowledge Discovery and Data Mining*, pages 397–406. Association for Computing Machinery, 2015.

Lei Han and Yu Zhang. Multi-Stage Multi-Task Learning with Reduced Rank. In *Proceedings of the AAAI Conference on Artificial Intelligence*, volume 30, 2016.

Hongliang He, Wenyu Zhang, and Shuai Zhang. A novel ensemble method for credit scoring: Adaption of different imbalance ratios. *Expert Systems with Applications*, 98:105–117, 2018.

Pratik Kumar Jawanpuria, Maksim Lapin, Matthias Hein, and Bernt Schiele. Efficient Output Kernel Learning for Multiple Tasks. In *Advances in Neural Information Processing Systems*, volume 28. Curran Associates, Inc., 2015.

Jiahui Jiang, Ruimin Wang, Mengdi Wang, Kaifu Gao, Duc Duy Nguyen, and Guo-Wei Wei. Boosting Tree-Assisted Multitask Deep Learning for Small Scientific Datasets. *Journal of Chemical Information and Modeling*, 60(3): 1235–1244, 2020a.

Jian Jiang, Rui Wang, Menglun Wang, Kaifu Gao, Duc Duy Nguyen, and Guo-Wei Wei. Boosting tree-assisted multitask deep learning for small scientific datasets. *Journal of chemical information and modeling*, 60(3):1235–1244, 2020b.

Tsuyoshi Kato, Hisashi Kashima, Masashi Sugiyama, and Kiyoshi Asai. Multi-Task Learning via Conic Programming. In *Advances in Neural Information Processing Systems*, volume 20. Curran Associates, Inc., 2007.

Guolin Ke, Qi Meng, Thomas Finley, Taifeng Wang, Wei Chen, Weidong Ma, Qiwei Ye, and Tie-Yan Liu. LightGBM: A Highly Efficient Gradient Boosting Decision Tree. In *Advances in Neural Information Processing Systems*, volume 30. Curran Associates, Inc., 2017.

Azal Ahmad Khan, Omkar Chaudhari, and Rohitash Chandra. A review of ensemble learning and data augmentation models for class imbalanced problems: Combination, implementation and evaluation. *Expert Systems with Applications*, 244:122778, 2024.

Balaji Lakshminarayanan, Alexander Pritzel, and Charles Blundell. Simple and Scalable Predictive Uncertainty Estimation using Deep Ensembles. In *Advances in Neural Information Processing Systems*, volume 30. Curran Associates, Inc., 2017.

Peter J. Lenk, Wayne S. DeSarbo, Paul E. Green, and Martin R. Young. Hierarchical Bayes Conjoint Analysis: Recovery of Partworth Heterogeneity from Reduced Experimental Designs. *Marketing Science*, 15(2):173–191, 1996.

Sijin LI, Zhi-Qiang Liu, and Antoni B. Chan. Heterogeneous Multi-task Learning for Human Pose Estimation with Deep Convolutional Neural Network. In *Proceedings of the IEEE Conference on Computer Vision and Pattern Recognition (CVPR) Workshops*, pages 482–489, 2014.

Ya Li, Xinmei Tian, Tongliang Liu, and Dacheng Tao. Multi-Task Model and Feature Joint Learning. In *IJCAI*, pages 3643–3649, 2015.

Xuejun Liao and Lawrence Carin. Radial Basis Function Network for Multi-task Learning. In *Advances in Neural Information Processing Systems*, volume 18. MIT Press, 2005.

Haizhou Liu, Xuan Zhang, Hongbin Sun, and Mohammad Shahidehpour. Boosted Multi-Task Learning for Inter-District Collaborative Load Forecasting. *IEEE Transactions on Smart Grid*, 15(1):973–986, 2024a.

Lizhen Liu, Xiao Hu, Wei Song, Ruiji Fu, Ting Liu, and Guoping Hu. Neural Multitask Learning for Simile Recognition. In *Proceedings of the 2018 Conference on Empirical Methods in Natural Language Processing*, pages 1543–1553. Association for Computational Linguistics, 2018.

Qidong Liu, Xian Wu, Xiangyu Zhao, Yuanshao Zhu, Derong Xu, Feng Tian, and Yefeng Zheng. When MOE Meets LLMs: Parameter Efficient Fine-tuning for Multi-task Medical Applications. In *Proceedings of the 47th International ACM SIGIR Conference on Research and Development in Information Retrieval*, pages 1104–1114. Association for Computing Machinery, 2024b.

Wu Liu, Tao Mei, Yongdong Zhang, Cherry Che, and Jiebo Luo. Multi-Task Deep Visual-Semantic Embedding for Video Thumbnail Selection. In *Proceedings of the IEEE Conference on Computer Vision and Pattern Recognition (CVPR)*, pages 3707–3715, 2015.

Handong Ma, Zhecheng Dong, Mingcheng Chen, Wenbo Sheng, Yao Li, Weinan Zhang, Shaodian Zhang, and Yong Yu. A gradient boosting tree model for multi-department venous thromboembolism risk assessment with imbalanced data. *Journal of Biomedical Informatics*, 134:104210, 2022.

Aakarsh Malhotra, Mayank Vatsa, and Richa Singh. Dropped Scheduled Task: Mitigating Negative Transfer in Multi-task Learning using Dynamic Task Dropping. *Transactions on Machine Learning Research*, 2023.

Duncan McElfresh, Sujay Khandagale, Jonathan Valverde, Vishak Prasad C, Ganesh Ramakrishnan, Micah Goldblum, and Colin White. When Do Neural Nets Outperform Boosted Trees on Tabular Data? In *Advances in Neural Information Processing Systems*, volume 36, pages 76336–76369. Curran Associates, Inc., 2023.

Ishan Misra, Abhinav Shrivastava, Abhinav Gupta, and Martial Hebert. Cross-Stitch Networks for Multi-Task Learning. In *Proceedings of the IEEE Conference on Computer Vision and Pattern Recognition (CVPR)*, June 2016.

S. Moro, R. Laureano, and P. Cortez. Using Data Mining for Bank Direct Marketing: An Application of the CRISP-DM Methodology. In *Proceedings of the European Simulation and Modelling Conference - ESM'2011*, pages 117–121. EUROSIS, 2011.

Warwick Nash, Tracy Sellers, Simon Talbot, Andrew Cawthorn, and Wes Ford. Abalone. <https://archive.ics.uci.edu>, 1994.

Alexey Natekin and Alois Knoll. Gradient boosting machines, a tutorial. *Frontiers in Neurorobotics*, Volume 7 - 2013, 2013.

Luca Oneto, Michele Donini, Amon Elders, and Massimiliano Pontil. Taking Advantage of Multitask Learning for Fair Classification. In *Proceedings of the 2019 AAAI/ACM Conference on AI, Ethics, and Society*, pages 227–237. Association for Computing Machinery, 2019.

Shibin Parameswaran and Kilian Q Weinberger. Large Margin Multi-Task Metric Learning. In *Advances in Neural Information Processing Systems*, volume 23. Curran Associates, Inc., 2010.

Fabian Pedregosa, Gaël Varoquaux, Alexandre Gramfort, Vincent Michel, Bertrand Thirion, Olivier Grisel, Mathieu Blondel, Peter Prettenhofer, Ron Weiss, Vincent Dubourg, et al. Scikit-learn: Machine learning in Python. *the Journal of machine Learning research*, 12:2825–2830, 2011.

Antonella Plaia, Simona Buscemi, Johannes Fürnkranz, and Eneldo Loza Mencía. Comparing Boosting and Bagging for Decision Trees of Rankings. *Journal of Classification*, 39(1):78–99, 2022.

Liudmila Prokhorenkova, Gleb Gusev, Aleksandr Vorobev, Anna Veronika Dorogush, and Andrey Gulin. CatBoost: unbiased boosting with categorical features. In *Advances in Neural Information Processing Systems*, volume 31. Curran Associates, Inc., 2018.

Ali Rahimi and Benjamin Recht. Random Features for Large-Scale Kernel Machines. In *Advances in Neural Information Processing Systems*, volume 20. Curran Associates, Inc., 2007.

Manar D. Samad, Sakib Abrar, and Norou Diawara. Missing value estimation using clustering and deep learning within multiple imputation framework. *Knowledge-Based Systems*, 249:108968, 2022.

Sheng Shen, Shijia Yang, Tianjun Zhang, Bohan Zhai, Joseph E. Gonzalez, Kurt Keutzer, and Trevor Darrell. Multitask Vision-Language Prompt Tuning. In *Proceedings of the IEEE/CVF Winter Conference on Applications of Computer Vision (WACV)*, pages 5656–5667, 2024.

Yusuke Shinohara. Adversarial multi-task learning of deep neural networks for robust speech recognition. In *Inter-speech*, pages 2369–2372, 2016.

Ravid Shwartz-Ziv and Amitai Armon. Tabular data: Deep learning is not all you need. *Information Fusion*, 81: 84–90, 2022.

Tomáš Souček, Jean-Baptiste Alayrac, Antoine Miech, Ivan Laptev, and Josef Sivic. Multi-Task Learning of Object States and State-Modifying Actions From Web Videos. *IEEE Transactions on Pattern Analysis and Machine Intelligence*, 46(7):5114–5130, 2024.

Saravanan Srinivasan, Parthasarathy Ramadass, Sandeep Kumar Mathivanan, Karthikeyan Panneer Selvam, Basu Dev Shivaahare, and Mohd Asif Shah. Detection of Parkinson disease using multiclass machine learning approach. *Scientific Reports*, 14(1):13813, 2024.

C. De Stefano, M. Maniaci, F. Fontanella, and A. Scotto di Freca. Reliable writer identification in medieval manuscripts through page layout features: The “Avila” Bible case. *Engineering Applications of Artificial Intelligence*, 72:99–110, 2018.

Altyeb Altaher Taha and Sharaf Jameel Malebary. An Intelligent Approach to Credit Card Fraud Detection Using an Optimized Light Gradient Boosting Machine. *IEEE Access*, 8:25579–25587, 2020.

Sebastian Thrun and Joseph O’Sullivan. Discovering structure in multiple learning tasks: The TC algorithm. In *ICML*, volume 96, pages 489–497. Citeseer, 1996.

Samir Touzani, Jessica Granderson, and Samuel Fernandes. Gradient boosting machine for modeling the energy consumption of commercial buildings. *Energy and Buildings*, 158:1533–1543, 2018.

Hsinhan Tsai, Ta-Wei Yang, Tien-Yi Wu, Ya-Chi Tu, Cheng-Lung Chen, and Cheng-Fu Chou. Multitask learning multimodal network for chronic disease prediction. *Scientific Reports*, 15(1):15468, 2025.

Athanasis Tsanas and Max Little. Parkinsons Telemonitoring. <https://archive.ics.uci.edu>, 2009.

Simon Vandenhende, Stamatios Georgoulis, Wouter Van Gansbeke, Marc Proesmans, Dengxin Dai, and Luc Van Gool. Multi-Task Learning for Dense Prediction Tasks: A Survey. *IEEE Transactions on Pattern Analysis and Machine Intelligence*, 44(7):3614–3633, 2022.

Qi Wang, Yue Ma, Kun Zhao, and Yingjie Tian. A Comprehensive Survey of Loss Functions in Machine Learning. *Annals of Data Science*, 9(2):187–212, 2022a.

Sinan Wang, Yumeng Li, Hongyan Li, Tanchao Zhu, Zhao Li, and Wenwu Ou. Multi-Task Learning with Calibrated Mixture of Insightful Experts. In *2022 IEEE 38th International Conference on Data Engineering (ICDE)*, pages 3307–3319, 2022b.

Yuyan Wang, Xuezhi Wang, Alex Beutel, Flavien Prost, Jilin Chen, and Ed H. Chi. Understanding and Improving Fairness-Accuracy Trade-offs in Multi-Task Learning. In *Proceedings of the 27th ACM SIGKDD Conference on Knowledge Discovery & Data Mining*, pages 1748–1757. Association for Computing Machinery, 2021.

James Wilson, Viacheslav Borovitskiy, Alexander Terenin, Peter Mostowsky, and Marc Deisenroth. Efficiently sampling functions from Gaussian process posteriors. In *International Conference on Machine Learning*, pages 10292–10302, 2020.

Guoxuan Xia and Christos-Savvas Bouganis. Window-Based Early-Exit Cascades for Uncertainty Estimation: When Deep Ensembles are More Efficient than Single Models. In *Proceedings of the IEEE/CVF International Conference on Computer Vision (ICCV)*, pages 17368–17380, 2023.

Cemal Yilmaz, Hamdi Tolga Kahraman, and Salih Söyler. Passive Mine Detection and Classification Method Based on Hybrid Model. *IEEE Access*, 6:47870–47888, 2018.

ZhenZhe Ying, Zhuoer Xu, Zhifeng Li, Weiqiang Wang, and Changhua Meng. MT-GBM: A Multi-Task Gradient Boosting Machine with Shared Decision Trees. arXiv, 2022.

Shipeng Yu, Volker Tresp, and Kai Yu. Robust multi-task learning with t-processes. In *Proceedings of the 24th International Conference on Machine Learning*, pages 1103–1110. Association for Computing Machinery, 2007.

Wenchao Zhang, Peixin Shi, Pengjiao Jia, and Xiaoqi Zhou. A novel gradient boosting approach for imbalanced regression. *Neurocomputing*, 601:128091, 2024.

Wenlu Zhang, Rongjian Li, Tao Zeng, Qian Sun, Sudhir Kumar, Jieping Ye, and Shuiwang Ji. Deep Model Based Transfer and Multi-Task Learning for Biological Image Analysis. In *Proceedings of the 21th ACM SIGKDD International Conference on Knowledge Discovery and Data Mining*, pages 1475–1484. Association for Computing Machinery, 2015.

Ya-Lin Zhang and Longfei Li. Interpretable MTL from Heterogeneous Domains using Boosted Tree. In *Proceedings of the 28th ACM International Conference on Information and Knowledge Management*, pages 2053–2056. Association for Computing Machinery, 2019.

Yu Zhang and Qiang Yang. A Survey on Multi-Task Learning. *IEEE Transactions on Knowledge and Data Engineering*, 34(12):5586–5609, 2022.

Yu Zhang and Dit-Yan Yeung. Multi-Task Boosting by Exploiting Task Relationships. In *Machine Learning and Knowledge Discovery in Databases*, pages 697–710. Springer Berlin Heidelberg, 2012.

Zhanpeng Zhang, Ping Luo, Chen Change Loy, and Xiaoou Tang. Facial Landmark Detection by Deep Multi-task Learning. In *Computer Vision – ECCV 2014*, pages 94–108. Springer International Publishing, 2014.

Zhendong Zhang and Cheolkon Jung. GBDT-MO: Gradient-Boosted Decision Trees for Multiple Outputs. *IEEE Transactions on Neural Networks and Learning Systems*, 32(7):3156–3167, 2021.

Mengchen Zhao, Bo An, Yaodong Yu, Sulin Liu, and Sinno Pan. Data Poisoning Attacks on Multi-Task Relationship Learning. volume 32, 2018.

Zhi-Hua Zhou. *Ensemble methods: foundations and algorithms*. CRC press, 2012.

Maciej Zięba, Sebastian K. Tomczak, and Jakub M. Tomczak. Ensemble boosted trees with synthetic features generation in application to bankruptcy prediction. *Expert Systems with Applications*, 58:93–101, 2016.

Aybike Özyüksel Çiftçioğlu. RAGN-L: A stacked ensemble learning technique for classification of Fire-Resistant columns. *Expert Systems with Applications*, 240:122491, 2024.